

# *Electronics* **COOLING**

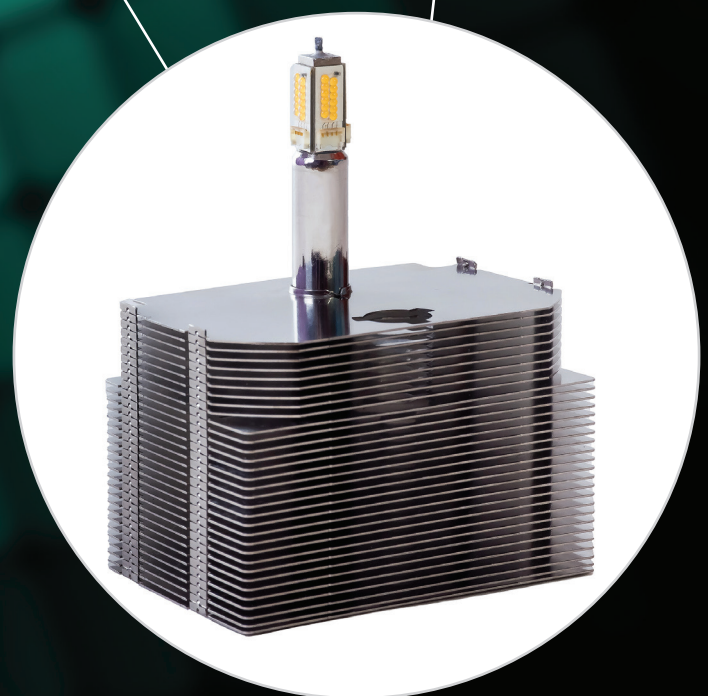
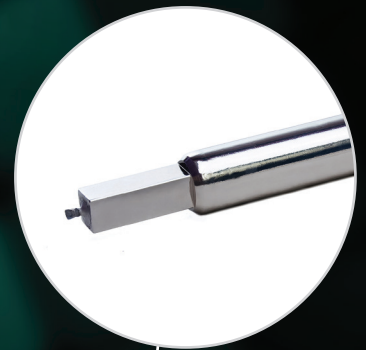
SEPTEMBER 2016  
electronics-cooling.com

## DESIGN CONSIDERATIONS WHEN USING HEAT PIPES

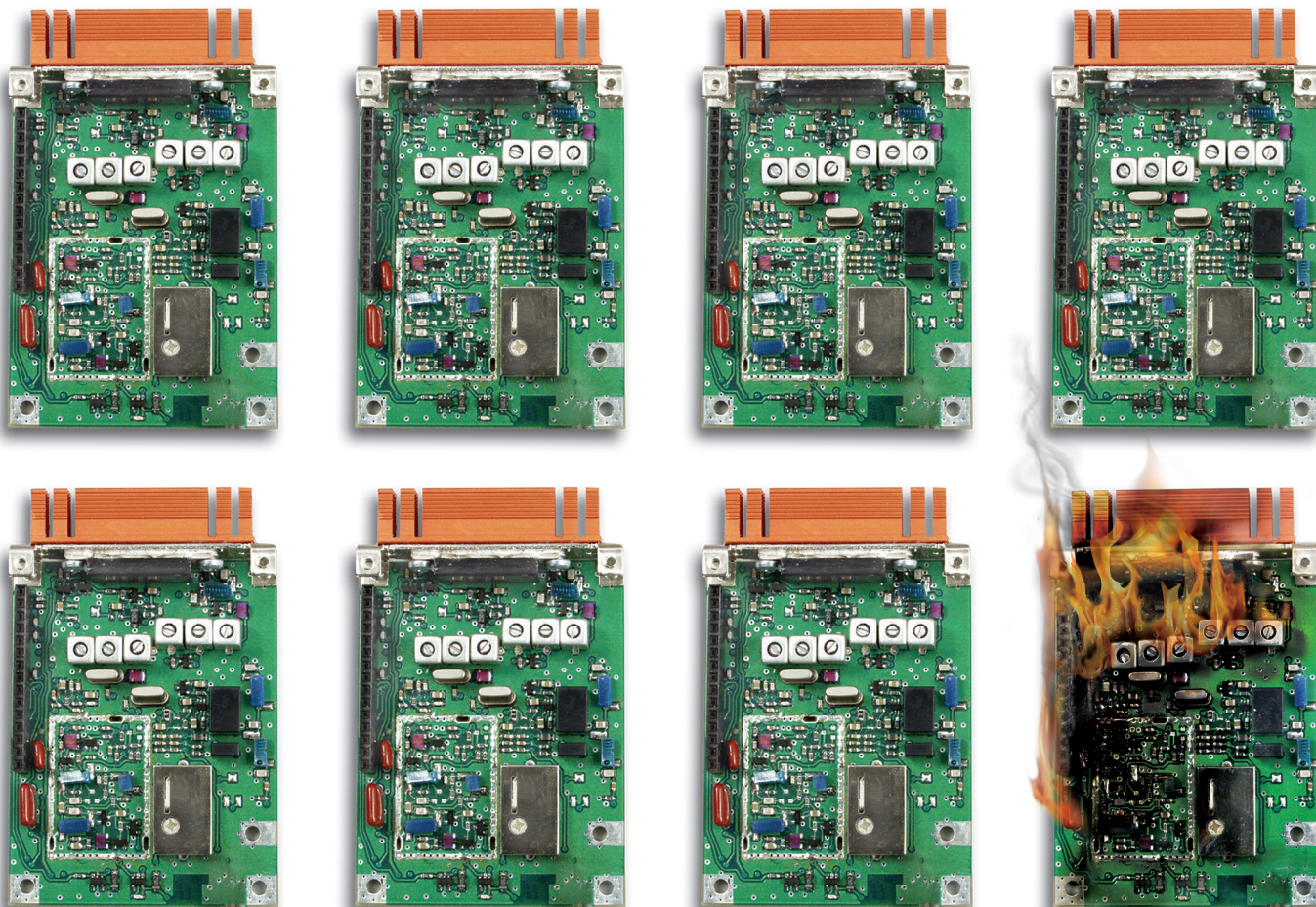


Pluggable Optics Modules -  
Thermal Specifications: Part 2

Comparison of Heatsinks Used for the  
Thermal Management of LEDs







# 7 out of 8 electronic devices recommend Bergquist Thermal Clad® Substrates

(The 8th device was unavailable for comment)

## World leading OEMs choose Bergquist.

For 25+ years Thermal Clad® has been effectively used in industries such as high-power LED lighting, automotive, power conversion, motor control, aerospace/military, computer, telecommunications and more.

## Don't get burned - Choose your insulated metal substrates carefully.

Bergquist supplies the world with some of the best solutions in the business:

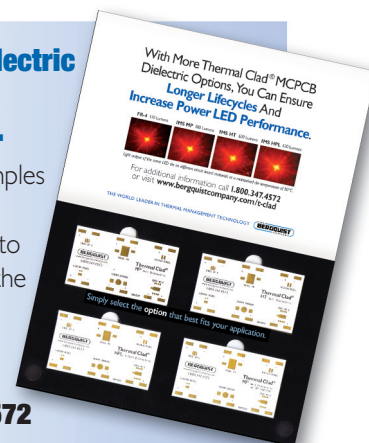
- Long-term dielectric strength
- Low thermal impedance
- U.L. Listed, high maximum operating temperature
- Long-term temperature testing

## Explore your dielectric options with a FREE Sample Kit.

This kit contains samples of select Bergquist Thermal Substrates to allow you to select the best option that fits your application.

To receive your kit, call **1-800-347-4572**

or qualify online at **[www.bergquistcompany.com/coolkit](http://www.bergquistcompany.com/coolkit)**



**[www.bergquistcompany.com](http://www.bergquistcompany.com) 1.800.347.4572**

9 5 2 . 8 3 5 . 2 3 2 2 f a x 9 5 2 . 8 3 5 . 0 4 3 0

18930 West 78th Street • Chanhassen, Minnesota 55317

**BERGQUIST**

# CONTENTS

**Electronics  
COOLING**

www.electronics-cooling.com

## 2 EDITORIAL

How to Define and Evaluate Research Impact

**Peter Rodgers**

*Editor-in-Chief, September 2016*

## 4 COOLING MATTERS

News of Thermal Management Technologies

## 8 CALCULATION CORNER

Spreadsheet-based Matrix Analysis – Extension to Transient Analysis

**Ross Wilcoxon, Ph.D.,**

*Associate Technical Editor*

## 13 THERMAL FACTS & FAIRY TALES

Fairy Tales About Heat Sink Performance Calculations

**Clemens J.M. Lasance,**

*Guest Editor, Philips Research Emeritus, Consultant@SomelikeitCool*

## 18 TECH BRIEF

Commercially-available Thermally Enhanced Polymer

Composite Materials Characteristics

**Peter Rodgers, Editor**

**Valérie Eveloy, The Petroleum Institute**

## 22 FEATURE ARTICLE

Comparison of Heatsinks Used for The Thermal Management of LEDs

**James Pryde<sup>1,2</sup>, David Whalley<sup>1</sup>, Weeratunge Malalasekera<sup>1</sup>**

<sup>1</sup>Loughborough University

<sup>2</sup>Tamlite Lighting, Redditch

## 29 FEATURE ARTICLE

Pluggable Optics Modules - Thermal Specifications: Part 2

**Terence Graham and Bonnie Mack,**

*Ciena Corporation*

## 34 FEATURE ARTICLE

Design Considerations when using Heat Pipes

**George Meyer,**

*Celsia Inc.*

## 40 INDEX OF ADVERTISERS

### Cover Picture

ETC Source Four® lighting fixture featuring its newly released 155 watt LED light engine (Source 4WRD™) which is as bright as a 575 watt HPL extended-life lamp. The 12mm diameter nickel plated heat pipe used in the thermal assembly is square at one end to allow 4-sided mounting of the LEDs and is now manufactured by Celsia Inc.

### ASSOCIATE TECHNICAL EDITORS

**Bruce Guenin, Ph.D.**

Principal Hardware Engineer, Oracle  
bruce.guenin@oracle.com

**Peter Rodgers, Ph.D.**

Associate VP Research Engagement,  
The Petroleum Institute  
prodgers@pi.ac.ae

**Ross Wilcoxon, Ph.D.**

Principal Mechanical Engineer,  
Rockwell Collins Advanced Technology Center  
ross.wilcoxon@rockwellcollins.com

### PUBLISHED BY

ITEM Media

1000 Germantown Pike, F-2  
Plymouth Meeting, PA 19462 USA  
Phone: +1 484-688-0300; Fax: +1 484-688-0303  
info@electronics-cooling.com  
electronics-cooling.com

### CONTENT MANAGER

Geoffrey Forman | geoff@item.media

### ASSISTANT EDITOR

Shannon O'Connor | shannon@item.media

### GRAPHIC DESIGN

Charlotte Higgins | charloette@item.media

### ASSISTANT MARKETING MANAGER

Chris Bower | chris@item.media

### MARKETING COORDINATOR

Erica Osting | erica@item.media

### PRODUCTION SPECIALIST

Evan Barr | evan@item.media

### Sr. BUSINESS DEVELOPMENT MANAGER

Janet Ward | jan@item.media

### BUSINESS DEVELOPMENT MANAGER

Todd Rodeghiero | todd@item.media

### ADMINISTRATIVE MANAGER

Eileen Ambler | eileen@item.media

### CIRCULATION ASSISTANT

Mary Ann Flocco | maryann@item.media

### CHIEF MEDIA OFFICER

Graham Kilshaw | graham@item.media

### ACCOUNTING ASSISTANT

Susan Kavetski | susan@item.media

### REPRINTS

Reprints are available on a custom basis at reasonable prices in quantities of 500 or more. Please call +1 484-688-0300.

### SUBSCRIPTIONS

Subscriptions are free. Subscribe online at [www.electronics-cooling.com](http://www.electronics-cooling.com). For subscription changes email [info@electronics-cooling.com](mailto:info@electronics-cooling.com).

All rights reserved. No part of this publication may be reproduced or transmitted in any form or by any means, electronic, mechanical, photocopying, recording or otherwise, or stored in a retrieval system of any nature, without the prior written permission of the publishers (except in accordance with the Copyright Designs and Patents Act 1988).

The opinions expressed in the articles, letters and other contributions included in this publication are those of the authors and the publication of such articles, letters or other contributions does not necessarily imply that such opinions are those of the publisher. In addition, the publishers cannot accept any responsibility for any legal or other consequences which may arise directly or indirectly as a result of the use or adaptation of any of the material or information in this publication.

ElectronicsCooling is a trademark of Mentor Graphics Corporation and its use is licensed to ITEM. ITEM is solely responsible for all content published, linked to, or otherwise presented in conjunction with the ElectronicsCooling trademark.





# EDITORIAL

## How to Define and Evaluate Research Impact

Peter Rodgers, Editor-in-Chief, September 2016



Over the last three years I have had the opportunity to author several editorials of *ElectronicsCooling* that articulated my thoughts to the electronics thermal management community. Topics have included the need for improvements on the dissemination of ongoing knowledge and the embracement of sustainable design practices. One editorial also queried if graduate engineers are being effectively educated for today's workplace. In equal measure, another editorial highlighted how much electronics thermal management, as a discipline, has evolved over the past twenty years, to now play an integral role of the product design process in most organizations. As this will be my last editorial, I deliberated on what should be its theme. As responsible for research engagement in a university, it became evident that the present theme should relate to the "burning" topic of research impact, which is open to interpretation, depending if one is based in academia or industry.

For a young academic, research impact may be harshly quantified via his/her *h*-index, a metric that attempts to measure both the productivity and citation impact of his/her publications. For academics, it may lead to an ivory tower mentality and the proliferation of least publishable unit (LPU) strategy, for which the minimum amount of information is used to generate a publication. For industry, especially in the current economic climate, management may qualify research impact in terms of its "*bang for the buck*." The long-term wellbeing of the organization may be at stake based on this Research & Development (R&D) strategy. Both approaches are flawed if utilized as ultimate benchmarks. In this regard, this editorial discusses on how to bridge this potential divide.

As a starting point, an appropriate definition is required for research impact. According to the Australian Research Council "*Research impact is the demonstrable contribution that research makes to the economy, society, culture, national security, public policy or services, health, the environment, or quality of life, beyond contributions to academia*" [1]. However how can research impact be best measured? As noted in [2], "*the impact of some research is evident immediately, whereas in other cases it can take years, or even decades, before the true value becomes apparent*." Unfortunately there are no simple *a priori* predictors of potential benefit or outcomes, and no single measure of impact. Consequently the path between a discovery generated from basic/fundamental research to its commercialization is generally strewn with significant roadblocks, the most infamous being the "valley of death." Its symbolism represents either poor research strategy, i.e. relevance, priority, and novelty not effectively considered from the onset, or insufficient funding for advancement of new knowledge towards piloting, deployment, and/or commercialization.

To avoid this, an institution, be it academic or industrial, needs to develop and execute a detailed implementation plan so that the

research, innovation and deployment strategy delivers the intended outcomes. In addition, it needs to implement and monitor policies in support of the development, dissemination and monitoring of research impact. By doing so, the odds of successfully investing in knowledge creation and supporting its commercialization can be considerably improved. This is why joint industry projects (JIPs) still offer one of the most effective routes to carry out ambitious R&D that spreads the costs over the participating parties. In parallel, funding agencies can focus on supporting research which increases our fundamental understanding in a domain of activity. With this approach, academics will avoid LPU strategy to the benefit of industry, who will ultimately receive their "*bang for the buck*."

### CHANGING OF THE GUARD

I wish to express my gratitude and honor to have served as a technical editor for *ElectronicsCooling* since 2013. Unfortunately, the future responsibilities of my day job will no longer make it feasible for me to provide the continued level of support necessary to assist the technical editorial team going forward. Therefore, it is with regret that I will step aside after the December edition. In this regard, I wish to commend ITEM Media for their commitment to the publication of *ElectronicsCooling*, by far one of the best trade magazines, and their hands off approach with its editorial content. During my tenure I thoroughly enjoyed the editorial process and the interaction with contributing authors. I will miss the collaboration with my fellow technical editors Bruce Guenin and Jim Wilson, the editorial skills of whom are greatly admired, in continually assisting authors to deliver a central message. Last but not least, thanks to you, the reader, for supporting *ElectronicsCooling*.

It is with pleasure to announce that Ross Wilcoxon has joined the technical editorial team. Ross has had a distinguished career in thermal engineering, and is currently a Principal Mechanical Engineer in the Rockwell Collins Advanced Technology Center. Ross conducts research and supports product development related to component reliability, electronics packaging and thermal management. He is a past Chair of the SEMI-THERM conference, has an extensive publication record and holds over thirty US patents. Prior to joining Rockwell Collins in 1998, Ross was an assistant professor at South Dakota State University. He received B.S. and M.S. degrees in mechanical engineering from South Dakota State University, and a Ph.D. in mechanical engineering from the University of Minnesota. Having known Ross personally for over twelve years, future editions of *ElectronicsCooling* will be in good hands, and we wish him and the team every success.

### REFERENCES

- [1] Australian Research Council, "Research Impact Principles and Framework," <http://www.arc.gov.au/research-impact-principles-and-framework>, accessed August 17, 2016.
- [2] University of Oxford, "Research Impact," <https://www.ox.ac.uk/research/research-impact?wssl=1>, accessed August 17, 2016.





# MARK YOUR CALENDAR

## October 4-6, 2016

Join us for

# THERMAL LIVE 2016

This free online event is an innovative concept in education and networking in thermal management.

Created for electronics and mechanical engineers, it provides tools to learn the latest in thermal management techniques and topics.

Produced by **Electronics Cooling®** magazine, Thermal Live™ features webinars, roundtables, whitepapers, and new in 2016, live product demonstrations.....  
and yes, there really is no cost to attend!

**[www.thermal.live](http://www.thermal.live)**

# COOLING MATTERS

## News of Thermal Management Technologies

### RESEARCH UNDERWAY FOR HEAT CONDUCTOR SUBSTITUTES FOR DIAMOND

(July 5, 2016) Thanks to a research grant awarded from the Office of Naval Research for pursuing “high risk-high reward” scientific and technological breakthroughs, six universities are working to develop cost-effective and high-quality substitutes for diamond as a heat conductor.

Diamond was recently discovered to be the best available heat conductor, however it is too rare and expensive to produce for “widespread applications,” warned Boston College News. Boston College Professor of Physics, David Broido, and the university team “will try to confirm the prediction made by Broido and collaborators that the compound, boron arsenide, can offer diamond-like performance at reasonable cost,” as part of this project.

“The team’s challenge is to make high quality boron arsenide, to confirm the performance predictions through measurements, and more broadly to understand heat flow in materials at a fundamental level,” said Broido to the Boston College News.

### COOLING POWERFUL ELECTRONICS WITH POWERFUL SAND

(July 13, 2016) Recently, associate professor Baratunde Cola of the Woodruff School of Mechanical Engineering at the Georgia Institute of Technology uncovered the “potential of silicon dioxide nanoparticles coated with a high dielectric constant polymer for cooling power-hungry electronic devices,” reported Hexus.net.

According to Hexus, “the cooling occurs as the result of a nanoscale electromagnetic effect created on the surface of these [silicon dioxide] ‘sand’ particles.” According to Professor Cola, “The nanoparticle effect increases the thermal conductivity of the particles 20-fold,” which is “enough of a boost to make this material to the ranks of *expensive polymer composites used for heat dissipation*.”

This material is “said to have the potential to outperform conventional heatsink materials,” reported Hexus.

### GOOGLE USES AI TO CONTROL COOLING IN DATA CENTERS

(July 20, 2016) Google has been using its newly acquired AI technology from DeepMind to reduce the amount of energy its data centers have been consuming.

“The AI technology is applied to the management of the servers and other electronics at the company’s proprietary data centres and is used specifically to fine-tune the cooling systems,” explained TheInquirer.net. DeepMind co-founder Demis Hassabis said, “It controls about 120 variables in the data centres. The fans and the cooling systems and so on [...]”

According to The Inquirer, “The software uses an adapted form of the machine learning software developed by DeepMind to play Atari 2600 video games. Deployed in the data centre, the software learns how the servers work and manipulates fans and other elements to reduce their use when not needed.”

DeepMind’s technology was “deployed in Google data centres only in recent months, but has already resulted in a 15 per cent improvement in power use efficiency,” reported The Inquirer.

## Datebook

Sept. 13 – 15

### PCB West 2016

Santa Clara, California  
<http://www.pcbwest.com/>

Sept. 13 – 15

### Electric & Hybrid Vehicle Technology Expo

Novi, Michigan  
<http://www.evtechexpo.com/>

Oct. 4 – 6

### Thermal Live 2016

Online  
<http://thermal.live>

Oct. 11 – 16

### iMAPS 2016

Pasadena, California  
<http://www.imaps.org/imaps2016/>

Oct. 25 – 27

### Advanced Technology Workshop and Tabletop Exhibit on Thermal Management

Los Gatos, California  
<http://www.imaps.org/thermal/>

Nov. 8 – 11

### Electronica 2016

Munich, Germany  
<http://electronica.de/>

Nov. 16

### 2016 EMC Live Test Bootcamp

Online  
<http://tb.emclive2016.com>

Dec. 1 – 2

### ETA 2016

Berlin, Germany  
<https://www.iav.com/us/events/iav-conferences/1st-eta-conference-i-energy-and-thermal-management-air-conditioning-waste>



## THERMAL EXPANSION DISCOVERY COULD LEAD TO MORE DURABLE ELECTRONICS

(June 27, 2016) Stanford professor of materials science and engineering, Reinhold Dauskardt, and doctoral candidate Joseph Burg, recently released a study revealing that the layers protecting transistors in chips respond differently to compression and tension of bending and stretching.

"It has always been assumed that these dense insulating materials react exactly the same way to being pushed as they do when pulled, as when they expand due to heat," said Dauskardt, "We found that they are actually stiffer when compressed than when stretched, and we can use this knowledge to design more durable chips and devices."

According to Stanford News, the materials' response to expansion and contraction is "inherently related to the interaction within the network of particular atoms or groups of atoms – known as terminal groups – that do not fully bond during production."

Stanford News explained, "In compression, these terminal groups strongly repel each other to make the network stiffer. In tension, like weak links in a chain, their failure to bond causes these very same atoms to interact less, making the materials less stiff and, consequently, to expand more than expected as they heat up."

This research paper titled "Elastic and Thermal Expansion Asymmetry in Dense Molecular Materials" was published in the journal *Nature Materials*.

## COMBINATION OF TWO INSULATORS COULD ENABLE MORE EFFICIENT HEAT MANAGEMENT

(July 28, 2016) Recently, "researchers at the University of Utah and the University of Minnesota have discovered that when two oxide compounds—strontium titanate (STO) and neodymium titanate (NTO)—are joined together, they make an extraordinary conductive material that could vastly improve power transistors," according to Spectrum.IEEE.org.

By themselves, each material operates as an insulator, but together, researchers have shown they are "up to five times more conductive than silicon," reported Spectrum IEEE, "[...] scientists found that the bonds between the atoms from the oxide compounds arrange themselves in a way that generates 100 times more free electrons than conventional semiconductors, which means the new material can transport more electrical current."

Nanomaterials have been the great recent focus as a possible solution to heat management issues in electronics. Spectrum IEEE said, "By making more efficient power transistors, less power is wasted, and because wasted electricity is given off as heat, these devices will not run as hot as they have in the past."

The research is described in the journal *APL Materials*, but more research is needed.

## HEAT SINKS IMPROVED WITH 3D PRINTING

(July 18, 2016) The complimenting research done by Oak Ridge National Laboratory and the University of Tennessee Knoxville has found a way to improve the heat dissipation in electronics using 3D printing.

According to 3DPrint.com, "[Oak Ridge] researchers are showing that 3D printed aluminum may be a more viable source for conducting heat than traditional materials. And at [Tennessee], a team has taken on the challenge of making genetic algorithms that combined with the customization available through 3D printing, allow for better heatsinks."

"In comparing aluminum materials, the researchers compared thermal conductivity," 3DPrint.com reported, "Pitting the traditional 6061 aluminum heatsink (with <1% Si and 1.5% Mg) against one 3D printed through direct metal laser sintering by Linear Mold AMS (using 10% Si and 0.5% M), they found that the 3D printed model performed much better after [heat] treatment."

The 3D printed heat sink "rose to a permanent thermal conductivity of just under 200W/mK" from 180W/mK, according to 3DPrint.com.

The researchers then tested the performance of shapes and their designs by employing "their genetic design algorithms and finite element modeling in COMSOL software, using a 50kW water-cooled silicon carbide H-bridge inverter for electric vehicles as an example," reported 3DPrint.com. They printed another heat sink to compare with the reference, and evaluated their work through the badness function.

The results were a bit less than desirable, but the researchers concluded creating an improved 3D-printed heat sink is possible, although the "process may be changed in future work."

## LIQUID COOLED DATA CENTER WITH MORE POWER AND NO LEAKAGE

(June 29, 2016) Recently, eBay, Dell, and Intel claimed to have made "major strides in channeling the potential of liquid cooling" to enable greater processing power without excessive consumption "that could have implications for the hyperscale and web services market," according to EnterpriseTech.com

eBay, the world's largest online marketplace, which handles more than 1 billion transactions per day and has nearly 95 million global active users, has "made the decision to commit to water cooling in partnership with Dell and Intel" to "pack more power at a lower cost," reported EnterpriseTech.

"Key to the project is the anti-leakage provisions engineered into the liquid cooling capabilities of Triton [...], Dell's rack-scale infrastructure for hyperscale implementations, combined with a customized 200W Intel Xeon processor E5 v4, which provides significant performance increases over the highest performing Intel Xeon processor on the market today – and generates a lot of heat," explained EnterpriseTech, "The

result: according to Dell, Triton's ability to sub-cool the processor and operate at higher frequencies means it can deliver for similar costs nearly 60 percent greater performance than Intel's Xeon E5-2680 v4. Compared with average air-cooled data centers, Triton uses 97 percent less cooling power and has a power usage effectiveness (PUE) of 1.02 to 1.03."

Austin Shelnutt, principal thermal engineer at Dell, said, "We have a very elaborate leak mitigation system within the rack [...] that starts with every blade or server. We have leak detection and leak containment, and the ability to turn off water within the individual blades within the chassis itself, and the rack itself, depending on where a leak detection occurs, to isolate the splash zone."

Dell built the data center cooling solution that eBay will be using, claiming that, with Triton, it is the "first major vendor to safely bring facility water directly in each server sled to cool the CPU," delivering "cooling along with the lowest water consumption of any liquid cooled solution," according to EnterpriseTech.

# THERMAL LIVE 2016 SNEAK PEAK

OCTOBER 4 - 6, 2016

Online and free. Interactive Webinars, Roundtables, and more. Learn directly from thermal management thought leaders without leaving your seat.

## TECHNICAL PROGRAMS AND PRESENTER INFORMATION

### THERMAL LIVE 2016 PREVIEW

Below is a partial list of presenters and programs for Thermal Live 2016. Please visit [Thermal.Live](http://Thermal.Live) for a full list of presenters, programs, and additional information.



Speaker:  
**George Meyer**

This course is being taught by George Meyer, a thermal industry veteran with over three decades of experience in electronics thermal management. He holds over 70 patents in heat sink and heat pipe technologies and currently serves as the CEO of Celsia Inc.

#### Heat Pipes & Vapor Chambers – Useful Guidelines for Heat Sink Implementation

Webinar – Tuesday, October 4, 2016 | 12:15 PM – 1:00 PM

##### Overview:

Heat pipes, and increasingly vapor chambers, are common devices used to improve heat sink thermal performance by over 30% when compared to solid metal alternatives. This webinar will cover two-phase device similarities, differences, misconceptions, best uses, sizing and performance modeling through the presentation of numerous examples.

##### Who Should Attend:

Engineers interested in learning about how to best incorporate heat pipes and/or vapor chambers into their next heat sink design.



Speaker:  
**Chris Chapman**

Chris Chapman has worked in the electronics cooling industry for over 25 years and has been a key contributor for Aavid with many strategic customer programs. Currently Chris is the Director of Product Management, Two Phase, and Liquid Cooling Products.

#### The Fluid Network – Optimizing Hydraulic and Thermal Performance

Webinar – Wednesday, October 5, 2016 | 12:15 PM – 1:00 PM

##### Overview:

Although cold plates are a key component to a liquid cooled system, the fluid network also consists of pumps, heat exchangers, control instrumentation, quick disconnects, fittings, and tubing; all of which require careful planning and engineering. This presentation and discussion offer insights on how to plan and engineer a robust, reliable, and affordable liquid installation by optimizing both the subcomponents and the system as a whole.

##### Who Should Attend:

Program Managers, System Engineers & Component Engineers



## Increasing Product Reliability with Automated Thermal Model Calibration

Webinar – Thursday, October 6, 2016 | 12:15 PM – 1:00 PM

### Overview:

Electronics are designed into dynamic and often unpredictable environments. The dynamic thermal behavior of the device influences its operation, reliability, and ultimately the end-user experience. Failure to properly capture the dynamic thermal behavior leads to overdesign, more field failures, and longer design cycles. This session will introduce an automated method to calibrate thermal models against dynamic measurement.

### Who Should Attend:

Thermal Engineers, Reliability Engineers, Quality Engineers and Managers.



Speaker:  
**John Wilson**

John Wilson joined Mentor Graphics Corporation, Mechanical Analysis Division (formerly Flomerics Ltd) after receiving his BS and MS in Mechanical Engineering from the University of Colorado at Denver. Since joining in 1999, John has worked on or managed more than 70 thermal and airflow design projects. His modeling and design knowledge range from component level to data centers, heat sink optimization and compact model development.

John has extensive experience in IC package level test and analysis correlation through his work at Mentor Graphics' San Jose based Thermal Test Facility. He is currently the Consulting Engineering Manager in the Mechanical Analysis Division.

## Utilizing Thermoelectric Devices to Optimize Thermal Management Systems

Roundtable – Wednesday, October 5, 2016 | 1:30 PM – 2:15 PM

### Overview:

New products and applications require thermal management systems that push new limits of power density, effectiveness and environmental reliability. From outdoor electronics with strict temperature limits to microscale optical fiber components with exacting temperature control requirements, many applications demand thermal control beyond the capabilities of passive systems. On the other hand, environmental, size or noise constraints may preclude incorporating liquid or pumped refrigerant heat transfer systems in to applications. It turns out that thermal systems can be augmented and enhanced with thermoelectric devices, yet still maintain passive heat dissipation performance. In this seminar, Phononic will lead a discussion that educates the audience on application characteristics in which thermoelectric devices excel. We will also highlight application types where using thermoelectric heat pumps in the heat transfer system can unlock previously unattainable performance or features. Finally, we will share specific examples where smart thermal system design has combined with thermoelectric devices to solve unique end-product challenges.

### Who Should Attend:

All electronics engineers, mechanical engineers and thermal management professionals who are looking to improve their practical knowledge in the field of thermal management.



Speaker:  
**Chris Caylor**

Chris is the Technical Director of the Electronics Cooling Business Unit at Phononic. He earned his PhD in Chemistry from the University of California at Berkeley. He is an engineering, research and product leader with over 10+ years in managing engineering programs and teams. Chris also has 7+ years experience in winning and managing government programs from diverse sources such as DoD, DoE and DARPA, as well as commercial program management with defense contractors & automotive OEMs. Chris also has 5+ years of product development and business development experience in the alternative energy, cleantech and cold products space. Chris is a recognized leader in advanced thermoelectric materials systems and device integration as well as compound semiconductors (including group IV, II-VI, III-V and V-VI) and their deposition techniques.

## ADDITIONAL PRESENTATIONS BY



Our schedule is constantly being updated – sign up for notifications today!  
please visit <http://Thermal.Live> for more information

# Spreadsheet-based Matrix Analysis – Extension to Transient Analysis

**Ross Wilcoxon, Ph.D.**  
Associate Technical Editor

## Nomenclature

Symbol	Parameter	Units
$C_{ij}$	Nodal conductance between nodes i and j	W/K
$C_p$	Specific heat capacity	J/kg.K
$K_{i-j}$	Inverse resistance ( $=1/R$ ) between nodes i and j	W/K
$m$	Mass	kg
$mc_p$	Thermal inertia	J/K
$Q_i$	Heat dissipation in node i	W
$Q_i^*$	Boundary condition heat load at node i	W
$R_{i-j}$	Thermal resistance between nodes i and j	K/W
$t$	Time	sec
$T_{amb}$	Ambient temperature	°C
$T_i$	Temperature of node i	°C
$x,y,z$	Network resistance nodes	---

## INTRODUCTION

Over the years, a number of articles [1-3] published in *ElectronicsCooling* have described the use of thermal resistance networks to analyze electronic systems. The analysis of a thermal resistance network begins by defining discrete nodes that are connected with resistors, with the magnitude of a flow between nodes defined by the configuration and the values of the individual resistors. In a thermal analysis, the nodes represent individual regions of the system that are each assumed to have a uniform, or representative average, temperature within the region, while the resistances are the thermal resistances between the nodes. This article describes how a thermal resistance network analysis for determining steady state temperatures can also be used to predict transient temperatures.

As described in [1], an inverse matrix analysis is a method that can be used to solve for the heat flows and nodal temperatures in a thermal resistance network with known boundary conditions. Reference [2] describes a method for solving a given thermal resistance matrix using a spreadsheet, and automated methods for generating a resistance network in spreadsheets are outlined in [3].

To briefly review how a thermal resistance network is generated and analyzed, let us consider four nodes that are connected to each other with thermal resistances, with two of the nodes connected to the ambient air temperature ( $T_4$ ), as illustrated in *Figure 1*. This network represents heat transfer in a single board-mounted electronic component described in [1,2], with the heat dissipating die designated as node T1.



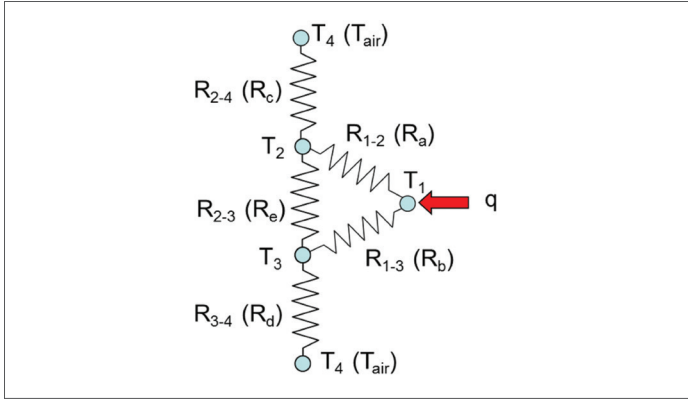


Figure 1. Four node thermal resistance network [2].

Under steady-state conditions, the energy that enters each node is equal to the energy that leaves it. The energy balance on node 1 can be written as:

$$Q_1 = T_1 * (K_{1-2} + K_{1-3}) - T_2 * K_{1-2} - T_3 * K_{1-3} = mc_p \frac{\partial T_1}{\partial t} \quad (1)$$

where  $Q$  is the external heat input to node 1 (*i.e.* power dissipation),  $T_x$  is the temperature of node  $x$ , and  $K_{x-y}$  is the thermal conductance between nodes  $x$  and  $y$ , *i.e.* the inverse of the thermal resistance.

For steady state conditions, the temperature does not change over time ( $\frac{\partial T}{\partial t} = 0$ ) and an energy balance can be applied to each body (*i.e.* node) with the three resulting equations written in matrix form:

$$\begin{bmatrix} K_{1-2} + K_{1-3} & -K_{1-2} & -K_{1-3} \\ -K_{1-2} & K_{2-1} + K_{2-3} & -K_{2-3} \\ -K_{1-3} & -K_{2-3} & K_{3-1} + K_{3-2} \end{bmatrix} \begin{bmatrix} T_1 \\ T_2 \\ T_3 \end{bmatrix} = \begin{bmatrix} Q_1^* \\ Q_2^* \\ Q_3^* \end{bmatrix} \quad (2)$$

where  $Q_i^* = Q_i + T_{amb}/R_{i-amb}$ ,  $T_{amb}$  is the ambient temperature, and  $R$  is the thermal resistance between the node and the ambient temperature.

Using the inverse matrix approach, the temperatures can be determined for a given set of specified boundary conditions (*i.e.* heat dissipation ( $Q$ ) values and one of the nodal temperatures). Equation (2) can be re-written as:

$$\begin{bmatrix} C_{11} & C_{12} & C_{13} \\ C_{12} & C_{22} & C_{23} \\ C_{13} & C_{23} & C_{33} \end{bmatrix} \begin{bmatrix} T_1 \\ T_2 \\ T_3 \end{bmatrix} = \begin{bmatrix} Q_1^* \\ Q_2^* \\ Q_3^* \end{bmatrix} \quad (2a)$$

where  $C_{ij} = -K_{i-j}$  (if  $i \neq j$ ),  $C_{ii} = \sum_{j=1}^n K_{i-j}$ , and  $i$  and  $j$  are nodes in the resistance network.

## TRANSIENT SOLUTION

The thermal resistance matrix solution can be extended to more complex systems with a larger number of nodes, and can be used to determine the steady state temperatures of a nodal system – assuming that the resistances between the nodes can be determined with sufficient accuracy. However, as presented in [1-3], it does not provide a method for

assessing the transient behavior of a system. The transient response of a node can again be determined by applying an energy balance to it, but in this case it is recognized that its temperature changes with time, as shown in Equation (1).

This same energy balance can be applied to each node in the thermal resistance network that includes thermal resistances between nodes and values of thermal inertia ( $mc_p$ ) for each node. A number of approaches can be used to solve the set of equations generated when Equation (3) is applied to each node in the network. For example, Guenin [4,5] compares the predictions of finite element modeling (FEM) to those of an analytical multi-stage resistor/capacitor network.

This article describes an alternative approach, using a simple numerical integration, for determining the transient behavior of a thermal resistance network solved using a spreadsheet analysis. The primary advantages to this approach are that it can added to a steady state analysis by using the same conductance matrix, and that it is relatively straightforward to account for power dissipation values that change with time and/or temperature.

As shown in Equation (3a), Equation (1) can be rewritten with finite changes in temperature and time, and is sufficiently accurate as long as the difference in time ( $\Delta t$ ) is small<sup>1</sup>. Equation (3a) can be rearranged into Equation (3b), in which  $T_{i,old}$  is the temperature of a node at a given time, and  $T_{i,new}$  is the temperature one time step,  $\Delta t$ , later:

(3a)

$$\frac{\{Q_1 + K_{1-amb} * T_{amb} - (T_1 * (K_{1-2} + K_{1-3}) - T_2 * K_{1-2} - T_3 * K_{1-3})\}}{m_1 c_{p,1}} = \frac{\partial T_1}{\partial t} = \frac{\Delta T}{\Delta t} \quad (3b)$$

$$\frac{\{Q_{1,old} + K_{1-amb} * T_{amb} - (T_{1,old} * (K_{1-2} + K_{1-3}) - T_{2,old} * K_{1-2} - T_{3,old} * K_{1-3})\}}{m_1 c_{p,1}} * \Delta t + T_{1,old} = T_{1,new}$$

It is apparent from comparing Equations (3b) and (2) that the conductance terms needed to solve for a temperature change are present in the conductance matrix used for the steady state analysis. If a spreadsheet has already been created to solve the steady state temperatures using an inverse matrix approach, the conductance matrix can also be used for transient analysis. This is relatively straight forward, particularly if one uses a somewhat convoluted function to simplify the conductance matrix.

To illustrate how to add a transient solution to an existing inverse-matrix resistance network solver, we will consider the four node model shown in Figure 1.

<sup>1</sup>How “small”  $\Delta T$  needs to be make the analysis “reasonably accurate” depends on the particular system being analyzed. The mass and specific heats of nodes and the rate at which power dissipations change over time can all influence how small of a time step is needed. If predicted results do not change significantly when the time step is reduced, the time step is probably sufficiently fine.

Figure 2 shows a matrix solution formulated in a spreadsheet for determining the steady state temperatures of the network shown in Figure 1.

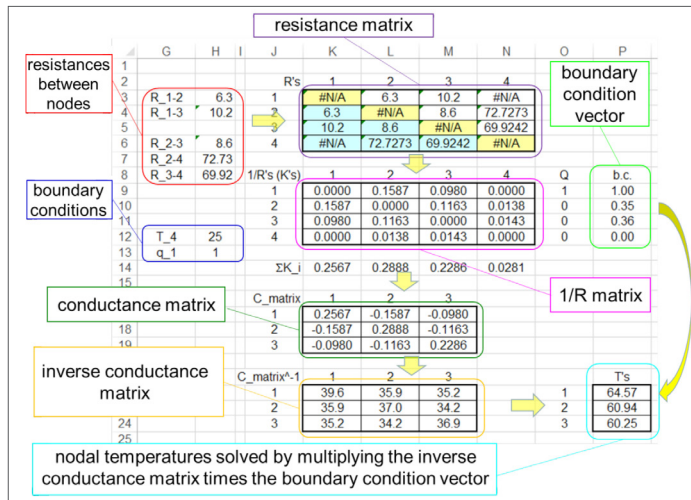


Figure 2. Spreadsheet procedure for solving nodal steady state temperatures of a thermal resistance network.

This analysis can be extended to find a transient solution as shown in Figure 3. This analysis begins by defining a time step value (shown in cell Q4) and defining columns for the power dissipation in each node (columns S, T and U). The transient time (column W) starts at 0, at which the nodes are all assumed to be at ambient temperature, T<sub>4</sub>. For this analysis, values of thermal inertia ( $mc_p$ ) of 0.5, 0.3, and 1.1 J/K were applied to nodes 1, 2, and 3, respectively (shown in cells X2 through Z2). These particular thermal inertia values were arbitrarily selected to allow the process to be demonstrated. The effects of ambient temperature were calculated in cells X1 through Z1 by multiplying the value of 1/R between each node and ambient times the ambient temperature.

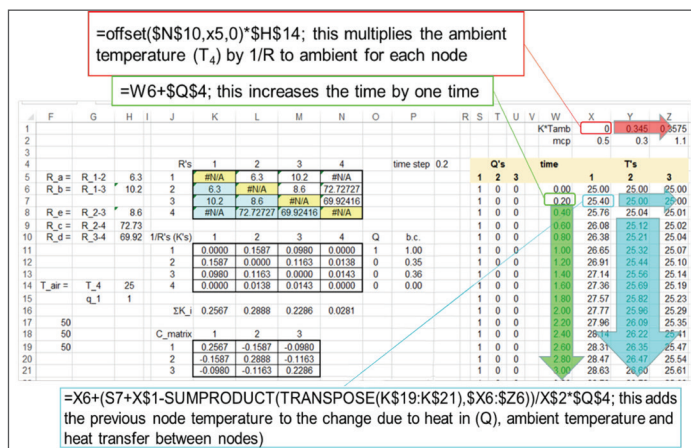


Figure 3. Spreadsheet procedure solution of thermal resistance network nodal transient temperatures obtained using numerical integration.

The somewhat convoluted function previously alluded to, was entered into cell X7 to calculate the temperature of node 1 after

the passage of one time step. This involved applying equation (3b) by adding the previous temperature in that node to the sum of: the heat dissipated in the node (in Cell S7), plus the value of  $K_{1-ambient} * T_{ambient}$  (Cell X\$1), plus each nodal temperature (at the previous time step multiplied by its corresponding value in the C matrix (i.e. conductance matrix); this sum was divided by the value of  $mc_p$  (X\$2) and multiplied by the time step (\$Q\$4). The 'TRANSPOSE()' function converts the column of values in the C matrix into a row that can be multiplied by the row of previous temperatures using the 'SUMPRODUCT()' function [6], which multiplies corresponding components in the given arrays, and returns the sum of those products.

Through careful use of absolute and relative referencing (defined by whether a "\$" sign is placed before a column and/or row reference), only three equations were typed into this portion of the spreadsheet and then copied to the rest of the columns or rows, as indicated in the block arrows. Note that since the TRANSPOSE() function is an array function, the equation must be entered with a Ctrl-Shift-Enter rather than simply the Enter key. Also, if changes are made to a cell with an array function, it may be necessary to firstly clear previous matrix equations from those cells before copying updated equations into them.

The resulting transient solution shows the temperature asymptote to the steady state temperatures of 64.6 °C, 60.9 °C and 60.3 °C for nodes 1, 2 and 3, respectively, that were predicted using the inverse matrix analysis, as shown in Figure 4. The specific values for thermal resistances and heat loads used in this analysis, Case 1, and an additional analysis, are summarized in Table 1.

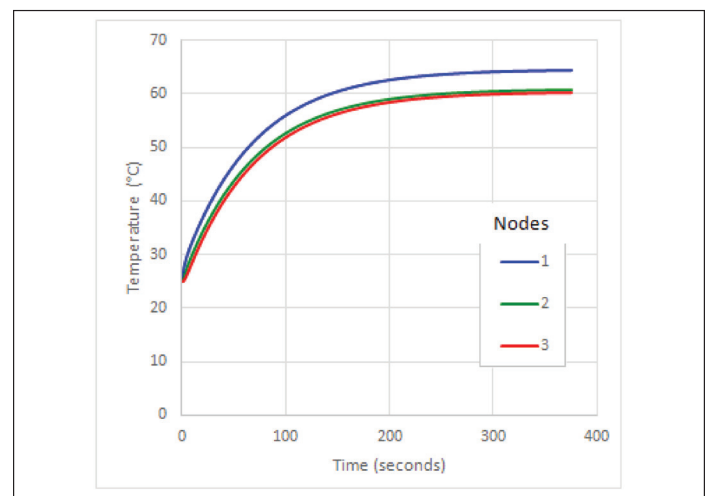


Figure 4. Thermal resistance network nodal transient temperature response for fixed heat dissipation (Case 1, Table 1).

The spreadsheet could have been slightly simplified by using fixed values for the power dissipation for each node, rather than using constant values assigned to the three columns (S,T and U). However, using the values in the individual columns does allow for the analysis to include temperature and/



or time-dependent power dissipation. For example, Figure 5 shows the transient temperatures for the same system when the power dissipation in node 1 was determined with the equation  $=\text{MAX}(0, 3*\sin(t/10))$ , to simulate a pulsed power dissipation, and the power dissipation of node 2, which was 0 in the previous analysis, was defined as  $0.1 * \sqrt{T_2/500}$ , to simulate a temperature dependent power dissipation. These equations were easily implemented into the existing columns for power dissipation.

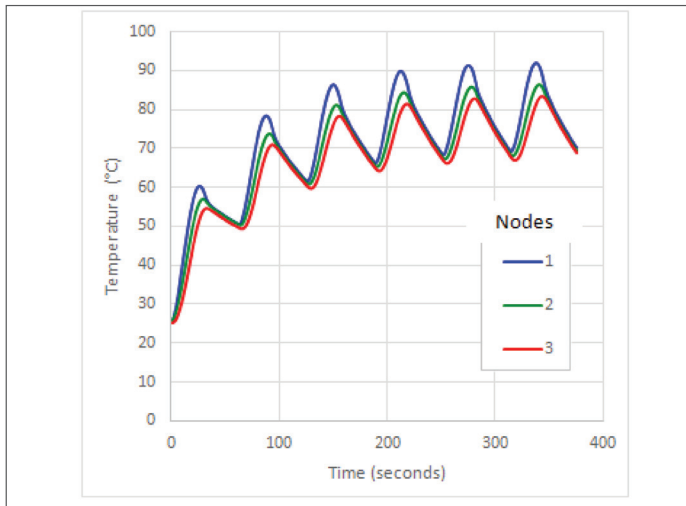


Figure 5. Thermal resistance network nodal transient temperature response for pulsed, temperature dependent heat dissipation (Case 2, Table 1).

Table 1. Input inverse thermal resistances and heat dissipations for nodal temperature prediction.

Node	Inverse Resistance, K to node				Nodal Heat Dissipation	
	1	2	3	4 (ambient)	Case 1	Case 2
1	n/a	6.3	01.2	$\infty$	1	$\text{MAX}(0, 3*\sin(t/10))$
2	6.3	n/a	8.6	72.73	0	$0.1 * \sqrt{T_2/500}$
3	10.2	8.6	n/a	69.92	0	0

Note: Nodal thermal resistance network shown in Figure 1.

## FINAL COMMENTS ON SPREADSHEET-BASED ANALYSIS

Spreadsheets are wonderful tools that can be used to analyze a wide variety of scientific problems. Even their most ardent supporters, however, will grudgingly admit that at some point there are better tools for analyzing complex systems. If a thermal analysis requires more than a dozen nodes to sufficiently describe a resistance network, it may be time (or past time) to consider using a dedicated analysis tool such as FEA software. As the number of cells in a spreadsheet grows, the chances for mistakes in typing, *etc.*, grow and the savings accomplished with a “quick and dirty” analysis can ultimately be quite expensive. Using “cookbook” approaches, such as what has been described in this article, can reduce the risk of user errors by limiting the number of different equations that need to be typed into the spreadsheet. However even with these approaches,

the spreadsheet analyst needs to be willing to admit when the complexity of a particular analysis has moved to the point at which other tools are more appropriate.

With that said, spreadsheet-based analysis can be extremely useful and can often accelerate the understanding of a situation. An additional advantage of spreadsheets is their transportability. In this author’s experience, there have been a number of cases in which customers (both internal and external) requested a tool to help them understand the impact of different decisions, rather than a static analysis of a given set of design decisions. Many of those customers did not have access to the necessary FEA tools or the knowledge to use them; however they all knew how to use a spreadsheet.

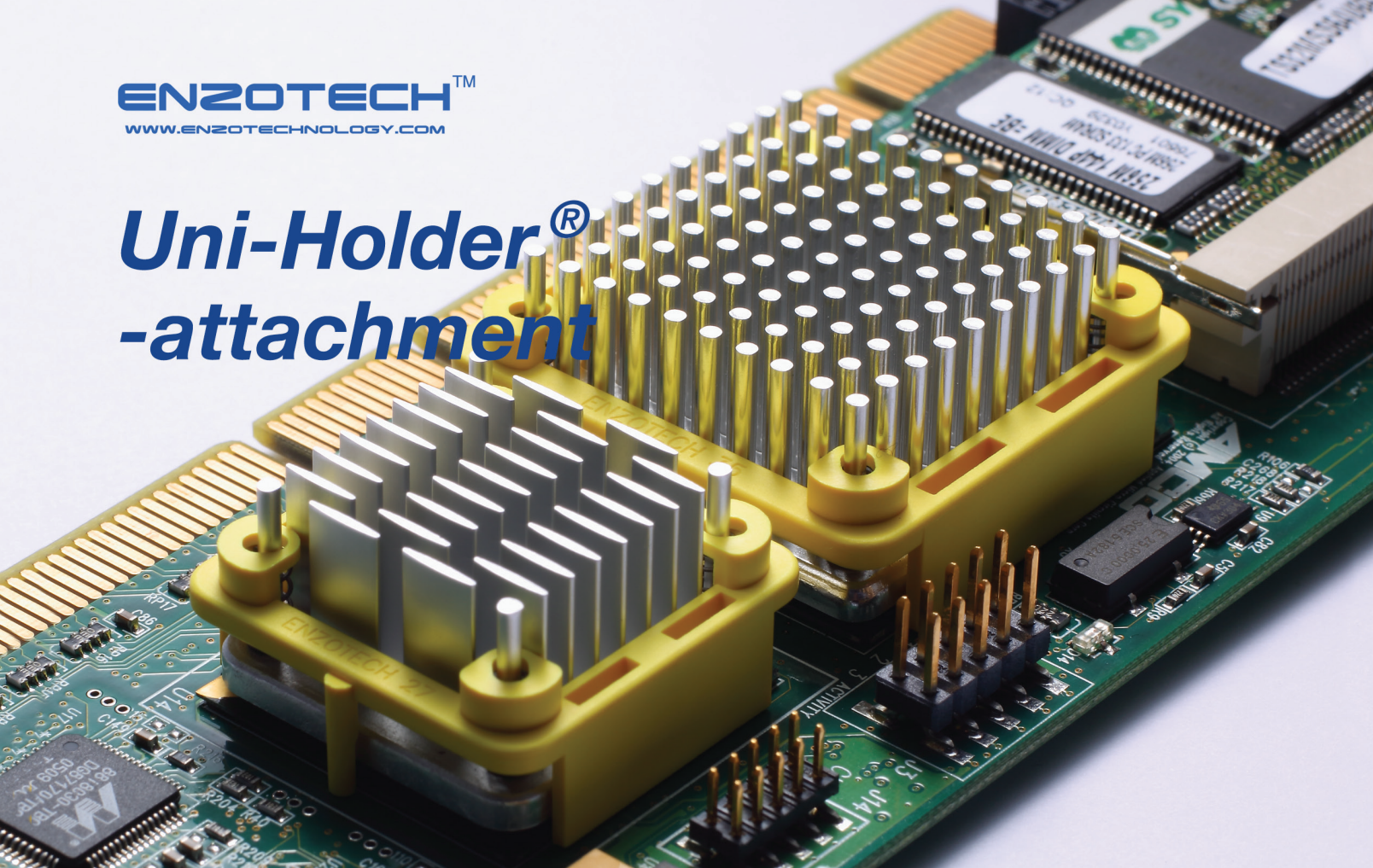
## REFERENCES

- [1] Simons, R., “Using a Matrix Inverse Method to Solve a Thermal Resistance Network,” *ElectronicsCooling*, June 2009, <http://www.electronics-cooling.com/2009/05/using-a-matrix-inverse-method-to-solve-a-thermal-resistance-network/>, accessed August 11, 2016.
- [2] Wilcoxon, R., “Calculation Corner: A Spreadsheet based Matrix Solution for a Thermal Resistance Network: Part 1,” *ElectronicsCooling*, September 2010, <http://www.electronics-cooling.com/2010/09/calculation-corner-a-spreadsheet-based-matrix-solution-for-a-thermal-resistance-network-part-1/>, accessed August 11, 2016.
- [3] Wilcoxon, R., “Spreadsheet Based Thermal Resistance Analysis Part 2: Generating the Thermal Resistance Matrix,” *ElectronicsCooling*, June 2011, <http://www.electronics-cooling.com/2011/06/spreadsheet-based-thermal-resistance-analysis-part-2-generating-the-thermal-resistance-matrix/>, accessed August 11, 2016.
- [4] Guenin, B., “Calculation Corner: Transient Thermal Modeling of a High-Power IC Package, Part 1,” *ElectronicsCooling*, December 2011, <http://www.electronics-cooling.com/2011/12/transient-modelling-of-a-high-power-ic-package-part-1/>, accessed August 11, 2016.
- [5] Guenin, B., “Calculation Corner: Transient Thermal Modeling of a High-Power IC Package, Part 2,” *ElectronicsCooling*, March 2012, <http://www.electronics-cooling.com/2012/03/calculation-corner-transient-modeling-of-a-high-power-ic-package-part-2/>, accessed August 11, 2016.
- [6] Microsoft Excel, “SUMPRODUCT function,” <https://support.office.com/en-us/article/SUMPRODUCT-function-16753e75-9f68-4874-94ac-4d2145a2fd2e>, accessed August 11, 2016.

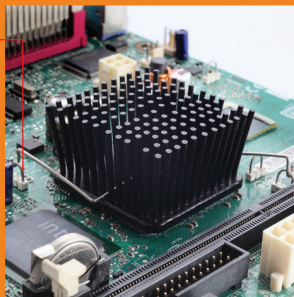
## CONTACT INFORMATION

**Ross Wilcoxon, Ph.D.,** | Principal Mechanical Engineer  
Advanced Technology Center | Rockwell Collins  
400 Collins Rd NE, MS 108-101, Cedar Rapids, IA 52498, USA  
Email: [ross.wilcoxon@rockwellcollins.com](mailto:ross.wilcoxon@rockwellcollins.com)

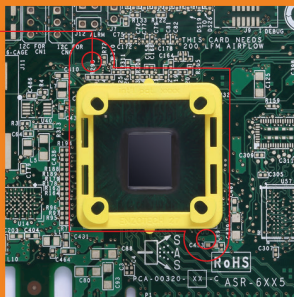
# Uni-Holder® -attachment



wire spring  
anchor  
pedestal



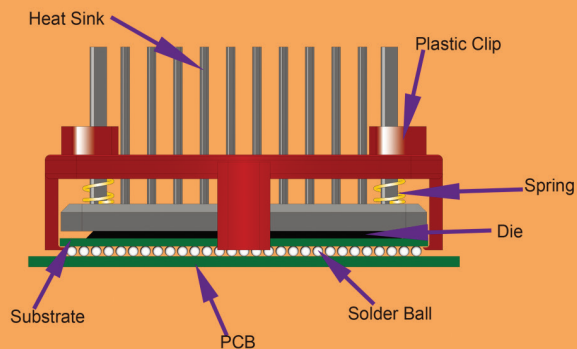
push pin  
hole



## SPACE IS MONEY

No mounting holes required ! Save precious PWB space for routing and components and not heat sink mounting holes.

Enzotech's Uni-Holder® Attachment can attach a heat sink as reliably as a push pin or Z-wire solution WITHOUT the needed thru holes.



Illustrations of Uni-Holder® attachment

## ENZOTECHNOLOGY CORP.

Address : 14776 Yorba Ct. Chino, CA 91710 USA

Tel : 909-993-5140

Fax : 909-993-5141

E-mail : [info@enzotechnology.com](mailto:info@enzotechnology.com)

Website : [www.enzotechnology.com](http://www.enzotechnology.com)



# Fairy Tales About Heat Sink Performance Calculations

Clemens J.M. Lasance,

Guest Editor, Philips Research Emeritus, Consultant@SomelikeitCool

When Peter Rodgers invited me to again write a Thermal Facts and Fairy Tales (TF&F) column, I immediately thought of a recent webinar on basic heat sink calculations that I attended, in order to get an idea of the current status-quo in these matters. Well, in my humble view there was room for improvement. Apart from certain minor issues, I was triggered by three topics that I felt were not treated in a correct way when dealing with practical situations, namely;

- (i) The fact that a heat sink does not only function as an area enlarger
- (ii) A much too simple explanation of the apparent (effective) emissivity of heat sinks
- (iii) The (mis)use of heat sink convective heat transfer correlations

With these three topics in mind, this TF&F column aims to outline my two cents on these issues.

## 1. A HEAT SINK HAS TWO FUNCTIONS

This topic has been treated in *extenso* in references [1,2], with a summary provided here. One should realize that a heat sink performs two very different functions:

- (i) Enlarge the surface area for heat transfer
- (ii) Spread the heat (providing a significant temperature gradient exists over the dissipating surface)

Suppose we wish to calculate the effect of a heat sink attached to an arbitrary generic electronic component without modeling all component-heat sink details. The first function is easy to address: simply multiply the real-life convective heat transfer coefficient by the area enlargement factor to obtain an effective heat transfer coefficient. It is the second function that can cause a problem when we need to consider the temperature gradient over the component surface that the heat sink is to be attached to. For this analysis, let's start by dividing the component surface into two areas: the central and periphery. When the heat sink is attached, the heat spreading reduces the maximum temperature of the central area and increases the minimum temperature in the peripheral region. This means that the effective heat transfer coefficient of the central area

(required to lower its temperature is through addition of the heat sink base only) is significantly increased. Reference [1] highlights this aspect when a considerable increase in the average central heat transfer coefficient results, compared to the overall average value, i.e.  $100 \text{ W/m}^2\text{K}$  versus  $8 \text{ W/m}^2\text{K}$ , for a natural convection application. In this context, if we want to generate a heat sink compact model to increase the efficiency of computational fluid dynamic (CFD) models, it is therefore mandatory to always explicitly model the heat sink base, with a compact description added for the remaining fin structure. Here is a first order estimation of this effect: suppose that for certain components that exhibit a significant surface temperature gradient, the central area is one quarter of the total area, and its effective heat transfer coefficient is 12 times higher than on the peripheral area, then the influence of the base is about as strong as a three-fold total area extension.

## 2. THE QUESTION ABOUT THE APPARENT EMISSIVITY OF HEAT SINKS

The analytical calculation of the apparent (or effective) emissivity (or emittance) of a heat sink can represent a significant effort as it depends strongly on the heat sink geometry. The apparent heat sink emissivity can be determined with high accuracy by employing radiation network theory, as discussed in pages 291-303 of reference [3]. However such calculations are no longer necessary in the age of computer-aided engineering software having embedded radiation calculation options. Let us define the heat sink geometry as shown in *Figure 1(a)*.

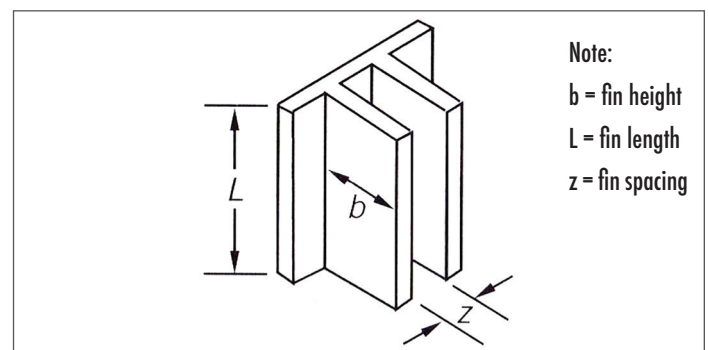


Figure 1(a) Heat Sink Geometry



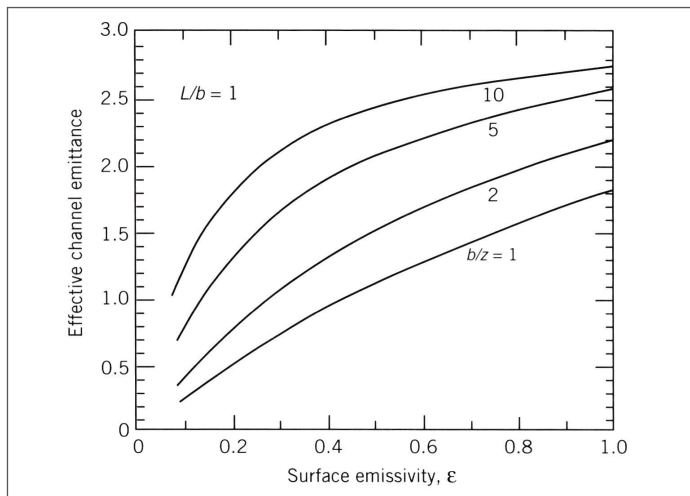


Figure 1(b) Channel radiative emittance for  $L/b = 1$ .

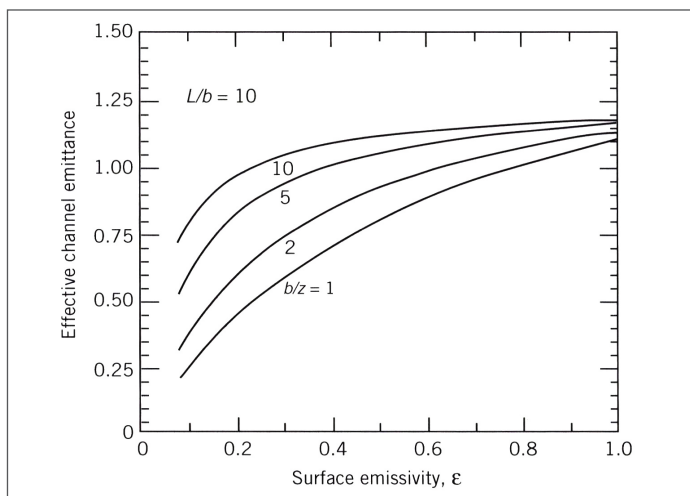


Figure 1(c) Channel radiative emittance for  $L/b = 10$ .

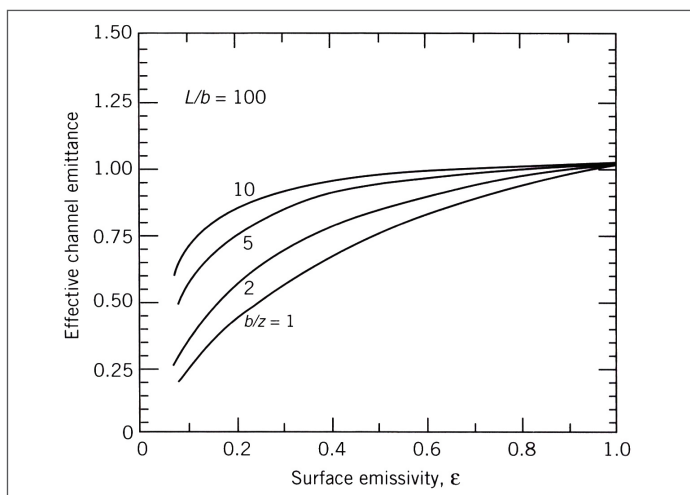


Figure 1(d) Channel radiative emittance for  $L/b = 100$ .

Figure 1. Effective (apparent) channel emittance (emissivity) for various heat sink geometries (taken from [3]).

The subsequent graphs shown in *Figures 1b to 1d* provide a realistic impression of what to expect. Herein the apparent emissivity is related to the base surface area without fins. For short and wide fins (e.g.  $L/b=1$ ,  $b/z=1$ ), it is obvious that a considerable part of the additional area is exposed to the environment, and hence its emissivity does matter. Furthermore, because of the extended surface area, the apparent emissivity can be greater than one because the base area is the reference. The opposite is true for long and closely-spaced fins (e.g.  $L/b=100$ ,  $b/z=10$ ); in this case its emissivity does not play any role, and the extended area from a radiation point of view is negligible. The point is that the radiation entering the fin channel cannot escape without multiple reflections between the fin channel surfaces. In addition, heat sinks with such a layout are only used for forced convection, hence the radiation contribution to the total heat transfer is minimal anyway. The conclusion must be: don't bother with emissivity calculation for forced convection applications, but do for natural convection, especially for those applications where often widely-spaced fins in a non-traditional shape are used, such as in the field of light emitting diode (LED) applications.

In summary, don't trust simple rules-of-thumb for natural convection applications. Caveat: check upfront if your application is really naturally-convection driven. In most cases you will conclude that we encounter buoyancy-induced forced convection [4]. When a heat sink has already been selected, a simple test is recommended: measure the operating temperature drop before and after painting the heat sink.

### 3. THE (MIS)USE OF HEAT SINK CORRELATIONS

The problems with convective heat transfer correlations for practical purposes are extensively discussed in references [5-7]. Let me quote (a bit adapted) from my TF&F column of June 2015 [7].

The background in a nutshell is that the handbooks showing impressive heat transfer correlations are inherently based upon a set of conditions/constraints that are not satisfied in real-life. When you believe in the following axioms, then the "Holy Books of Heat Transfer" are consistent and comprise a wealth of information, very useful for a basic understanding of the physics. Here are the underlying axioms:

- Uniform boundary conditions, either constant temperature or flux
- Uniform approach flow with a degree of turbulence as close as possible to zero (that's why research type wind tunnels are huge).
- (Very) simple geometries: smooth, flat and thin plates, parallel plate channels, pipes
- Single source, especially for natural convection
- Constant properties
- Fan dynamics based on air flow chamber testing
- Extended surfaces based on Murray-Gardner assumptions (see e.g. [8])

- “Complex shapes” means there exist an analytical solution
- Heat spreading limited to one-layer, one-sided heat transfer
- Radiation diffuse and grey

This means that if and only if the physical situation conforms to the assumptions does the experimenter have the right to assume that the predicted results will be obtained. That means much more than simply matching Nusselt (Nu) with Rayleigh (Ra) or Reynolds (Re) numbers. Specifically, most analytical (and numerical) studies assume uniform flow velocity with a specified turbulence (often zero), uniform temperature and the origins of the velocity boundary layer and the thermal boundary layer on the surface. For many fields of heat transfer, such as turbulence, boiling, heat exchangers, channel flow, *etc.*, these axioms form a sound base. **Not so for electronics cooling at the system level.**

Especially when referring to heat sinks, the author published a TF&F column titled “How useful are heat sink correlations” in [9]. Bottom line is that to use correlations to obtain a reasonable estimation of heat sink performance is a fairy tale. What’s wrong is that most equations are based on the following assumptions, in addition to the ones previously listed:

- Parallel plate heat sinks
- Fully ducted flow
- Fully developed flow
- Strong impact of 3D flow (especially in natural convection) not considered
- Equal number of fins and channels
- Negligible entrance and exit effects
- Laminar and uniform approach flow
- No temperature gradient in heat sink base
- Heat spreading effect of base not taken into account
- Uniform fin temperature (both between fins and within a fin)

Now, have a look at some state-of-the-art heat sink geometries for LED applications in **Figure 2**, in addition to the ones pictured in the December 2013 TF&F column [9].

Is there anyone out there who can tell me with a straight face that a Nusselt number correlation based on parallel-plate heat sinks will predict a realistic performance of these products? I don’t think so.

Obviously, if you use handbook equations to base your heat sink design upon, or to predict the performance of a selected heat sink type, chances are high that you may miss all of the heat sinks shown in **Figure 2**. Sure, extrusion-based parallel-plate heat sinks are the cheapest around, but they score badly when it comes to optimization of shape, weight, volume, and performance, especially regarding optimal fin thickness. And the final argument in favor of using CFD codes instead of correlations: 3D printing is a booming business, and

for sure parallel plates are not the ones that will be high on the list for optimization.



Figure 2. Non-parallel plate heat sink geometries for LED applications.

## An EPOXY that thinks of *everything*

### Supreme 3HTND-2DA

Ideal for die attach applications

One part compound

No mixing/freezing needed

Ideal dispensing profile

No tailing or bleed out

**MASTERBOND®**  
ADHESIVES | SEALANTS | COATINGS

**40 YEAR  
ANNIVERSARY**

www.masterbond.com

## CONCLUSION

The starting point for this column was my experience with a heat sink webinar. I was not happy with the approach that it was presented, and the reasons why have been outlined in this column.

To all who want to transfer basic heat sink knowledge: tell facts, not fairytales. The fact is that reality is complex. Basic heat transfer about conduction, convection and radiation: OK, but tell the attendees also that in order to realize a competitive edge in eventual sales, much more knowledge is needed than some limited and outdated design rules. Compare it with electronic design: nobody believes that one is capable of designing a functional printed circuit board (PCB) after attending a webinar of half an hour. After this column one should understand why it is not simple to assess heat sink performance, which should be the bottom line.

## REFERENCES

[1] Lasance, C.J.M., "The Influence of Various Common Assumptions on the Boundary-Condition-Independence of Compact Thermal Models," IEEE Transactions on Components and Packaging Technologies, Vol. 27, Issue 3, pp. 523 – 529 (2004).

[2] Lasance, C.J.M., "Heat Sink Basics from an Industrial Point of View," Chapter 9 in: Thermal Management of LED Applications: Volume 2 - Solid State Lighting Technology and Application, Lasance C.J.M. and Poppe A. (Eds), Springer, New York, USA, pp. 347-387 (2014).

[3] Kraus, A. and Bar-Cohen, A., Design and Analysis of Heat Sinks, Second Edition, John Wiley and Sons, New York, USA, pp. 291-303 (1997).

[4] Moffat, R.J. and Ortega, A., "Buoyancy Induced Forced Convection," Heat Transfer in Electronic Equipment, ASME, New York, US, HTD-Vol. 57, pp. 135-144 (1986).

[5] Lasance, C.J.M., "Sense and Nonsense of Heat Transfer Correlations Applied to Electronics Cooling," in Proceedings of the Sixth Conference on Thermal, Mechanical and Multiphysics Simulation and Experiments in Micro-Electronics and Micro-Systems (EuroSimE), Berlin, Germany, April 18-20, pp 8-16 (2005).

[6] Lasance, C.J.M., "Most of Us Live neither in Wind Tunnels nor in the World of Nusselt," *ElectronicsCooling*, June 2010, <http://www.electronics-cooling.com/2010/04/thermal-facts-and-fairy-tales-most-of-us-live-neither-in-wind-tunnels-nor-in-the-world-of-nusselt/>, accessed August 5, 2016.

[7] Lasance, C.J.M., "The Holy Books of Heat Transfer: Facts or Fairy Tales?" *ElectronicsCooling*, June 2015, <http://www.electronics-cooling.com/2015/05/the-holy-books-of-heat-transfer-facts-or-fairy-tales/>, accessed August 5, 2016.

[8] Kraus, A., Aziz, A., and Welty, J., Extended Surface Heat Transfer, A Wiley-Interscience Publication, John Wiley and Sons, New York, USA (2001).

[9] Lasance, C.J.M., "How Useful are Heat Sink Correlations for Design Purposes?" *ElectronicsCooling*, December 2013, <http://www.electronics-cooling.com/2013/12/heat-sink-correlations-design/>, accessed August 5, 2016.

## CONTACT INFORMATION

**Clemens J.M. Lasance**  
Consultant  
SomelikeitCool  
Nuenen, the Netherlands  
Email: [lasance@onsnet.net](mailto:lasance@onsnet.net)



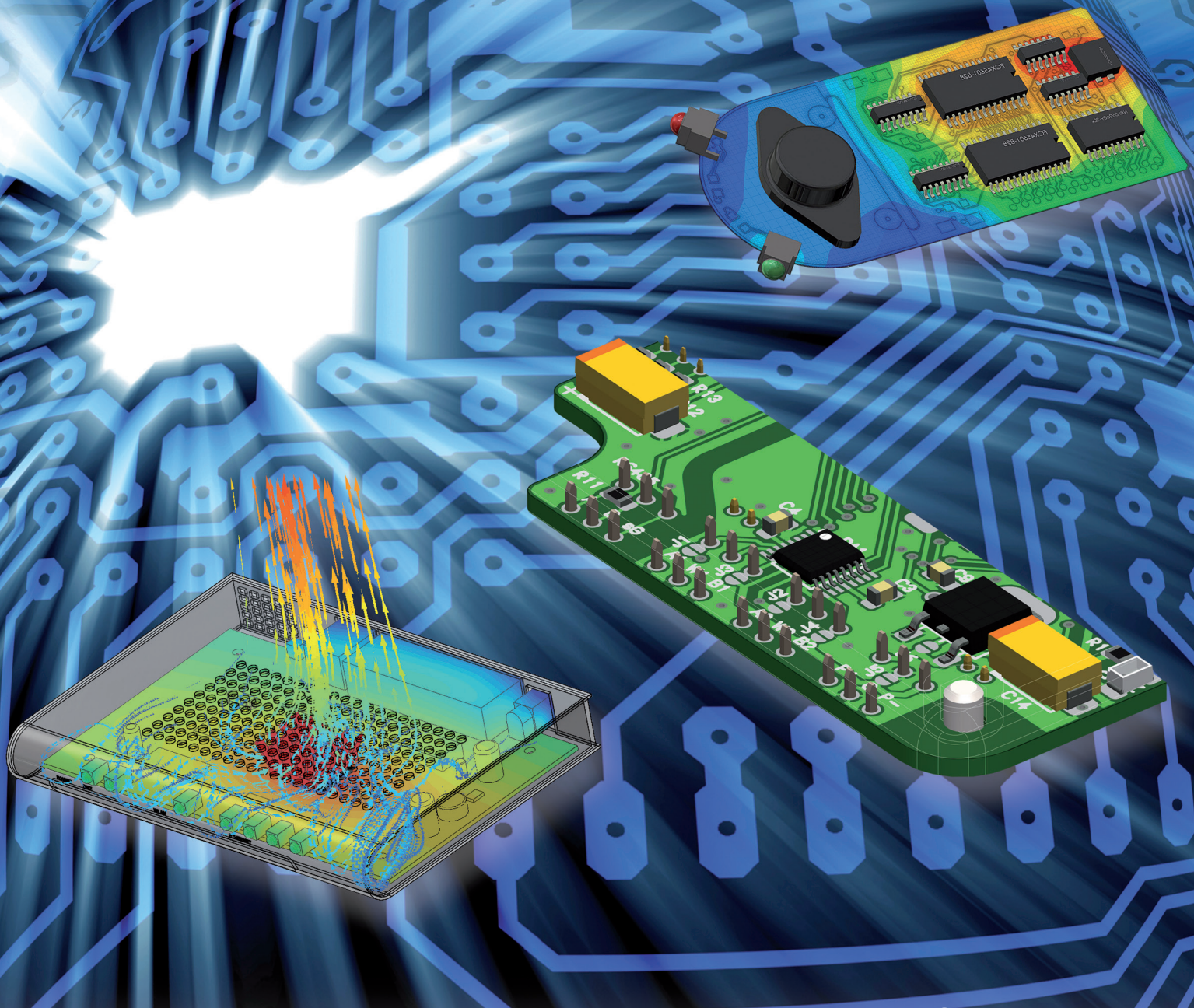
**STOP!** Look no further, we've got the solution to your thermal management needs...

**EDI CON**  
Electronic Design Innovation Conference  
September 20-22, 2016  
Boston, MA  
VISIT US AT BOOTH 223!

Get to know the **ThermaPlane™** by **ims**.  
Call today 401-683-9700

**ims**  
International Manufacturing Services, Inc.  
50 Schoolhouse Lane  
Portsmouth, RI 02871 USA  
[www.ims-resistors.com](http://www.ims-resistors.com) • [sales@ims-resistors.com](mailto:sales@ims-resistors.com)





# Learn to drive FloTHERM® XT

- With this hands-on virtual lab
- Become proficient using FloTHERM XT
- Create accurate thermal models in less time

Register Now for your instant 30 Day Free Trial  
[Go.mentor.com/flothermxt-vlab](http://Go.mentor.com/flothermxt-vlab)

**Mentor**  
**Graphics®**

— Mechanical Analysis

# Commercially-available Thermally Enhanced Polymer Composite Materials Characteristics

Peter Rodgers, Editor  
Valérie Eveloy, The Petroleum Institute

## INTRODUCTION

The development, characterization, and implementation of polymer composite materials for the thermal management of electronic equipment has recently begun to attract attention [1,2]. The enhanced thermal conductivity, low density, low cost, ease of manufacture and corrosion resistance of polymer composites make these materials attractive for the replacement of conventional heat sink and heat exchanger materials [3,4]. Polymer manufacturing is generally less expensive and energy-intensive than metal manufacturing [5]. Polymer low density also enables the manufacture of light structures that can facilitate assembly and transportation. Relative to standard polymers, composites have higher impact and yield strengths, higher temperature limits, and higher thermal conductivities [4]. The thermal and mechanical properties of the polymers are enhanced through the addition of fillers such as carbon fibers into the polymer matrix. The inclusion of up to 70% (volume %) carbon fibers, typically 100 to 300  $\mu\text{m}$  long, 10  $\mu\text{m}$  in diameter, having a thermal conductivity of up to 700 W/m.K, can increase polymer effective thermal conductivity from 0.5 to 30 W/m.K [6]. Thermally enhanced polymer composites

can enable innovative designs that may not be manufactured with metals, owing to the moldability and thus geometric flexibility of polymer composites. Polymer composites are particularly suited to air cooling applications characterized by a low Biot number (i.e., high convective thermal resistance relative to the internal conductive resistance). However, their properties depend upon the injection molding process parameters and can be highly anisotropic. Thus, the fibers ideally require to be oriented in the primary direction of conduction heat transfer. Although thermal conductivity is of importance, many other material properties need to be carefully considered for the selection of a polymer composite for a given application.

In this Tech Brief, which is an abridged version of the analysis published in [2], the mechanical and thermal properties of approximately thirty commercially available, injection moldable, thermally enhanced polymer composites are reviewed to guide the selection of candidate materials that could replace conventional metals in heat exchangers applications for microelectronics cooling.



DR. VALERIE  
EVELOY

is an Associate Professor of Mechanical Engineering at The Petroleum Institute, UAE. Previously, she was an Assistant Research Scientist at the University of Maryland, MD, USA, and Research Engineer at Nokia, Finland. Her present research interests include sustainable energy technologies, computational fluid dynamics, environmental emission dispersion, and polymeric heat exchangers. She has authored/co-authored over 90 refereed journal/conference publications, one book chapter, and co-edited the First and Second International Energy 2030 Conference proceedings. Dr. Eveloy is a member of international conference program committees focused on energy technologies, thermal phenomena in electronic systems; the EU-GCC Clean Energy Network II (2016–2018) and ASME.



## THERMAL AND MECHANICAL PROPERTIES

Current commercially-available, thermally enhanced polymer composite materials that can be injection molded, produced by six leading vendors, are compiled in *Table 1*. The majority of these materials use either polyamide 66 (PA 66) or Polyphenylene sulfide (PPS) as their matrix. For the purpose of non-commercialism, the vendors are anonymously designated throughout this article.

Polymer composite (abbreviation)	Vendor (abbreviation)
Polyamide (PA)	Vendor 1 (V1)
Polyamide 6 (PA 6)	Vendor 6 (V6), Vendor 4 (V4)
Polyamide 66 (PA 66)	Vendor 3 (V3), Vendor 2 (V2)
Polyphenylene sulfide (PPS)	Vendor 1 (V1), Vendor 3 (V3), Vendor 2 (V2), Vendor 6 (V6)
Polycarbonate (PC)	Vendor 5 (V5), Vendor 6 (V6)
Polyphthalamide (PPA)	Vendor 3 (V3), Vendor 1 (V1)
Liquid crystal polymer (LCP)	Vendor 1 (V1)
Polyamide 12 (PA 12)	Vendor 6 (V6)
Polybutylene terephthalate (PBT)	Vendor 6 (V6)
Polyaryletheretherketone (PEEK)	Vendor 6 (V6)
Polypropylene (PP)	Vendor 1 (V1)
Polypropylene Homopolymer (PPh)	Vendor 6 (V6)
Polyurethane (PU)	Vendor 6 (V6)

Before reviewing the properties of the materials listed in *Table 1*, the standards used for material characterization by the respective vendors were reviewed to ensure that the properties of polymer composites produced by different vendors can be compared on a like by like basis [2]. It was found that the standards used by the vendors are overall effectively equivalent.

A comparison of the thermal conductivity, tensile strength and modulus of the commercially-available polymer composites listed in *Table 1*, is presented in *Figure 1*. This comparison highlights that PA 66 group of materials have the highest thermal conductivity and tensile strength, and a high tensile modulus relative to other polymer composites.

A comparison of the flexural strength, flexural modulus and impact strength of the commercially-available polymer composites listed in *Table 1*, is presented in *Figure 2*. This data highlights that LCP has the highest flexural modulus (i.e., 32.3 MPa) and a good flexural strength. PA 66 materials have the highest flexural strength (179 - 193 MPa) and a good flexural modulus. Impact strength data for PA 66 from Vendor 3 is currently not available.

A comparison of the heat deflection temperature (HDT) and thermal conductivity of the commercially-available polymer composites at 1.8 MPa is presented in *Figure 3*. This data indicates that as thermal conductivity increases, the heat deflection temperature increases. PEEK has the highest HDT (i.e., 300 °C). Heat deflection temperature data is not available for PA 66 from Vendor 3.

Although not presented here in graphical format, a comparison of the density, elongation and mold shrinkage (both flow and cross-flow) of the commercially-available polymer composites listed in *Table 1* was also undertaken. Mold shrinkage is an important parameter to determine the molding process conditions. It was found that PA 66 has the greatest elongation (i.e., up to 1.5%), but no mold shrinkage data was reported for this material. On the other hand, PEEK and PA12 have a high mold shrinkage (flow 0.65%, cross-flow 0.8%).

The mechanical property data of commercially-available polymer composite materials reported in vendor documentation product data is typically limited to single values, with property anisotropy not documented. As highlighted in [7], anisotropy in mechanical properties can however have a significant impact on the mechanical integrity of heat exchanger applications.

*Table 2* summarizes the main results presented in *Figures 1* to 3. As indicated in *Table 2*, PA66 appears to have the best combination of thermal conductivity and mechanical properties. On the other hand, LCP has the highest tensile strength and flexural modulus, while PEEK has the highest heat deflection point.

*Table 3* compares the properties of the thermally enhanced composite polymers listed in *Table 1* with those of the corresponding standard (i.e., non-thermally enhanced) polymer matrices.

To illustrate the variation in thermal and mechanical properties of a given polymer composite matrix between vendors, a comparison of the thermal conductivity, tensile strength, flexural strength, tensile modulus and flexural modulus of PPS between Vendors V1 to V6 is presented in [2]. This data reveals that the thermal and mechanical properties of a given polymer composite matrix can vary considerably between vendors. In particular, significant differences in properties are observed between Vendors 1 and 3, who offer PPS materials having the same thermal conductivity. For example, product 11, V3 and product 10, V1, which both have a reported thermal conductivity of 20 W/m.K, exhibit 27%, 19% and 36 % difference in tensile strength, flexural strength and tensile modulus, respectively. This is possibly related to the type and quantity of filler used in each material.

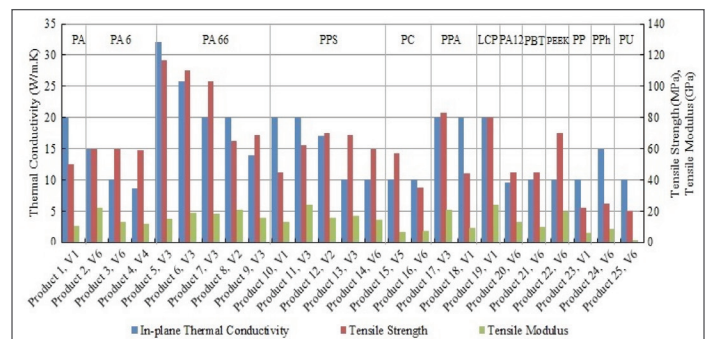


**Figure 1. Comparison of commercially-available polymer composite in-plane thermal conductivity ( $k$ ), tensile strength ( $\sigma_t$ ) and tensile modulus (ET). V1 to V6 refer to the product vendors listed in *Table 1* [2].**



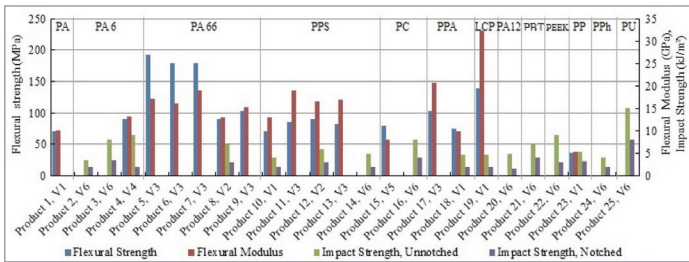
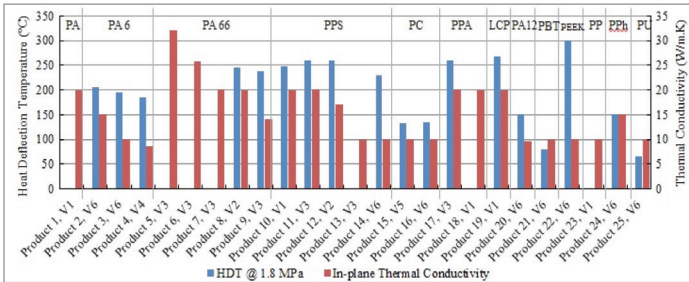


Figure 2. Comparison of polymer composite flexural strength ( $\sigma_f$ ), flexural modulus ( $E_f$ ) and impact strength. V1 to V6 refer to the product vendors listed in Table 1. Impact strength data for PA 66 from Vendor 3 currently not available [2].



Note: HDT = heat deflection temperature.

Figure 3. Comparison of polymer composite heat deflection temperature at 1.8 MPa and thermal conductivity. V1 to V6 refer to the product vendors listed in Table 1. Heat deflection temperature data not available for PA 66 from Vendor 3 [2].

Polymer Composite	Thermal Conductivity (W/mK)	Density (g/cc)	HDT @ 1.8 MPa (°C)	Tensile Strength (Mpa)	Tensile Modulus (Gpa)	Flexural Strength (Mpa)	Flexural Modulus (Gpa)	Elongation (%)
PA 66	20-32	1.59-1.82	238-248	65-117	14.8-20.7	90-193	13-17.2	0.75-1.5
PPS	10-20	1.7-1.8	230-260	45-70	13-24.1	70-90	13-19	0.31-0.75
PPA	20	1.56-1.7	260	44-83	9.07-20.7	75-103	9.84-20.7	0.563-1
LCP	20	1.84	268	80	24.3	139	32.3	0.25
PEEK	10	1.65	>300	70	19.5	Not reported	Not reported	0.5

Table Color Key

High	Medium	Low
------	--------	-----

Note: HDT = heat deflection temperature.

Properties	PA 66		PPS		PPA		LCP		PEEK	
	Std	Enh	Std	Enh	Std	Enh	Std	Enh	Std	Enh
Thermal Conductivity (W/mK)	0.24	20-32	0.08-0.29	10-20	0.15	20	0.0837	20	0.25	10
Density (g/cc)	1.13-1.15	1.59-1.82	1.35	1.7-1.8	1.15	1.56-1.7	1.35-1.84	1.84	1.31	1.65
HDT @ 1.8 MPa (°C)	70-100	238-248	100-135	230-260	117	260	180-355	268	160	>300
Tensile Strength (MPa)	95	65-117	48-86	45-70	76	44-83	110-186	80	70-103	70
Tensile Modulus (GPa)	1.59-3.79	14.8-20.7	3.45	13-24.1	2.41	9-21	9.7-19.3	24.3	3.6	19.5
Flexural Strength (MPa)	123	90-193	135	70-90	117.2	75-103	131-245	139	110.3	NR
Flexural Modulus (GPa)	2.83-3.24	13-17.2	3.96	13-19	2.53	10-21	12.2-18.6	32.3	3.86	NR
Elongation (%)	15-90	0.75-1.5	1-6	0.31-0.75	30	0.6-1.0	1.3-4.5	0.25	30-150	0.5

Note: Std = standard. Enh = enhanced. HDT = heat deflection temperature. NR = not reported.

## SUMMARY

Based on the data presented for commercially-available thermally enhanced polymer composite materials, polyamide 66 (PA 66) was found to have the best overall combination of thermal and mechanical properties at room temperature. Polyphenylene sulfide (PPS) also has a good combination of thermal and mechanical properties, and low processing conditions (e.g., temperature, pressure), but slightly lower mechanical properties. The material characterization data reviewed requires to be extended to conditions specific to electronic cooling applications, as well as to mechanical integrity, lifetime durability and material processability tests. The magnitude of polymer composite material mechanical property anisotropy for the materials considered in this study should also be investigated, as well as the impact of anisotropy on heat exchanger structural integrity.

## ACKNOWLEDGEMENTS

The financial support of ADNOC Research & Development Gas Sub-Committee is gratefully acknowledged.

## REFERENCES

- [1] Deisenroth, D.C. Arie, M.A., Dessiatoun, S., Shooshtari, A. Ohadi, M., and Bar-Cohen, A., 2015, "Review of Most Recent Progress on Development of Polymer Heat Exchangers for Thermal Management Applications," ASME 2015 International Technical Conference and Exhibition on Packaging and Integration of Electronic and Photonic Microsystems, San Francisco, California, USA, July 6–9, Paper No. IPACK2015-48637, 10 pages.
- [2] Evelyn, V., Rodgers, P., and Diana, A., "Performance Investigation of Thermally Enhanced Polymer Composite Materials for Microelectronics Cooling," Microelectronics Journal, Vol. 46, pp. 1216-1224 (2015).
- [3] Bahadur, R., and Bar-Cohen, A., "Orthotropic thermal conductivity effect on cylindrical pin fin heat transfer," International Journal of Heat and Mass Transfer, Vol. 50, pp. 1155–1162, 2007.
- [4] Cevallos, J.G., Bergles, A.E., Bar-Cohen, A., Rodgers, P., and Gupta, S.K., "Polymer Heat Exchangers - History, Opportunities, and Challenges," Heat Transfer Engineering, 33(13) pp. 1075-1093, 2012.
- [5] Luckow, P., Bar-Cohen, A., Rodgers P., and Cevallos, J., "Energy Efficient Polymers for Gas-Liquid Heat Exchangers," Journal of Energy Resources Technology, Vol. 132, pp. 021001-1/9, 2010.
- [6] Bahadur, R., "Characterization, Modeling and Optimization of Polymer Composite Pin Fins," Doctor of Philosophy Thesis, University of Maryland, College Park, MD, USA, 2005.
- [7] Robinson, F., Cevallos, J.G., Bar-Cohen A., and Bruck, H., "Modeling and Validation of a Prototype Thermally-Enhanced Polymer Heat Exchanger," Proceedings of the ASME 2011 International Mechanical Engineering Congress & Exposition (IMECE2011), November 11-17, 2011, Denver, Colorado, USA, Paper No. IMECE2011-65684.





Messe München

Connecting Global Competence

# Planet **e**: Where the future begins.

Automotive electronics of tomorrow. Today.

Automotive exhibition sector:  
**November 8–11, 2016**

**e**lectronica Automotive Forum:  
**November 8–11, 2016**

**e**lectronica Automotive Conference:  
**November 7, 2016**

All about **e**lectronica Automotive:  
[electronica.de/en/automotive](http://electronica.de/en/automotive)



Tickets & Registration: [electronica.de/en/tickets](http://electronica.de/en/tickets)

World's Leading Trade Fair for Electronic Components,  
Systems and Applications

Messe München | November 8–11, 2016 | [electronica.de](http://electronica.de)



**electronica** 2016  
inside tomorrow

# Comparison of Heatsinks used for the Thermal Management of LEDs

James Pryde<sup>1, 2</sup> David Whalley<sup>1</sup>, Weeratunge Malalasekera<sup>1</sup>

<sup>1</sup>Loughborough University

<sup>2</sup>Tamlite Lighting

## INTRODUCTION

The work of Kraus & Bar-Cohen [1] and Bar-Cohen *et al.* [2] provide a well-defined foundation for the design and optimisation of conventional heatsinks. However, advances in manufacturing processes and increasing access to simulation tools provide new opportunities to develop superior concepts. Comparing different heat sink design concepts, and consequently identifying the most effective design strategies, is a key requirement of development. In this regard, Lasance & Eggnik [3] propose an experimental method that incorporates metrics for ranking heatsink performance for given application. However, numerical methods of capturing a comprehensive, but simple assessment of thermal and hydraulic performance, are also required to support product development and promote the realisation of improved performance. The objective of this article is to establish suitable assessment criteria and apply them to the evaluation of various heatsink concepts for the passive cooling of light

emitting diodes (LEDs) used in general lighting applications. This was achieved with the aid of a commercially available computational fluid dynamic (CFD) simulation package.

It is important to relate the criteria on which the heatsink's performance is judged to the application. The LED is widely recognised as a revolutionary technology in the lighting sector. Its superior lifetime, energy consumption and quality of light is allowing it to rapidly displace established technologies [4]. However, heat (a waste product of their operation) compromises their reliability, efficiency and output characteristics [5]. Effective thermal management is consequently a critical aspect of their implementation. Studies from the US DOE [6,7] highlight the significant environmental benefits of LEDs, promoting their use alongside reliable and low energy consumption thermal management devices. For these reasons passively cooled heatsinks are particularly appropriate and so are the focus of this study.



**JAMES  
PRYDE**

Born in 1988 in Stafford, UK. He acquired an MSc degree in mechanical engineering at Staffordshire University in 2011. He has since been working in industry and is currently based at Tamlite Lighting (UK) as Senior Luminaire design engineer. In 2016 he became a chartered engineer with the Institute of Mechanical Engineers. Alongside working in industry he is pursuing a doctoral degree with Loughborough University where he is exploring appropriate thermal management techniques for LED luminaires within a commercial context.



**DAVID  
WHALLEY**

Born in Blackburn, Lancashire and attended Le-dbury Grammar School, Herefordshire. Graduated from Loughborough University in 1984 and subsequently worked as a research engineer both at Loughborough University and at the Lucas Advanced Engineering Centre in Solihull, Birmingham. Appointed as a lecturer in 1990 and promoted to Senior Lecturer in 1998. Visiting Professor, Chalmers University of Technology, Göteborg, Sweden and Nanyang Technological University, Singapore 2001/2002.



**WEERATUNGE  
MALALASEKERA**

Born in Sri Lanka, attended St. Thomas' College, Mount Lavinia, Colombo. University Education at University of Peradeniya, Sri Lanka, Graduated 1983. Obtained Ph.D. and D.I.C. from Imperial College of Science Technology and Medicine, University of London, 1988. 1984 - 85: Assistant Lecturer, Dept. of Mechanical Engineering, University of Peradeniya, Sri Lanka. 1985 - 89: Research Assistant/Post-doctoral RA (1989) at the Dept. of Mechanical Engineering, Imperial College, London. Joined Loughborough University as a lecturer in 1989.



## DEFINITIONS OF PERFORMANCE

Performance is an ambiguous term which can relate to; thermal conditions, material content, cost, manufacturability, aesthetics and environmental impact amongst many other parameters. For practical purposes it is necessary to restrict its definition to a few simple, but well defined, criteria.

First and foremost, the heatsink needs to facilitate sufficient transfer of heat to its environment. A common measurement of this property is the absolute thermal resistance, defined by the equation:

$$R_{\theta} = \frac{\Delta T}{Q} \quad (1)$$

where  $R_{\theta}$  is the thermal resistance ( $K.W^{-1}$ ),  $\Delta T$  is the temperature difference between the two reference points (K), and  $Q$  is the magnitude of thermal power transferred between these two points (W).

Absolute thermal resistance captures the combined effects of all heat transfer modes and associated thermal resistances so provides a useful assessment of thermal management capability. In this study thermal resistance was calculated between the peak heatsink temperature (i.e. base), and the ambient environment (i.e. far field quiescent air temperature).

Thermal resistance relates to specific load conditions. Models such as those developed by Sadeghi *et al.* [8] offer the necessary tools to compensate for different load conditions but tend to be complex. Standardised thermal load definitions (such as those proposed by Poppe *et al.* [9]) may be constrained when the application does not adhere to a standard configuration. However, it should be noted that transient thermal testing [10] is an invaluable tool for evaluating and validating thermal resistance characteristics but relies on physical specimen and specialist test equipment. For simulation it is often most practical to assess the thermal resistance characteristics of each case separately.

The same thermal resistance can be established by various heatsink designs, some of which may require less material or exploit superior geometry. Therefore a secondary measure of how effectively the heatsink design develops its thermal resistance is required. A heatsink employing high thermal conductivity material (aluminium in this study), proportionately large surface area and passive cooling is generally described by a small Biot number. Under this condition heat transfer is primarily governed by the body's interaction with the environment rather than internal conduction. As heat transfer to the environment is facilitated by the heatsink's surface, achieving the same thermal resistance using less surface area represents better utilisation of the heat transfer interface. A simple measure of effectiveness ( $E$ ) can therefore be estimated as:

$$E = R_{\theta} \times A \quad (2)$$

where  $A$  is the heatsink wetted surface area ( $m^2$ ). Effectiveness has the units  $m^2.K.W^{-1}$ , with smaller values representing

the combination of lowest thermal resistance achieved with the least surface area.

## HEATSINK CONCEPTS

Table 1 summarises a series of heatsink design concepts shown in Figure 1 which are considered in this study. The concepts cover a range of conventional and novel forms. This allows the performance of conventional forms (parallel plate, pin fin) to be benchmarked against verified references while the novel forms provide insight into previously unconsidered (to the author's knowledge) possibilities. The heatsink bounds were restricted to 60 x 65 x 65 mm (width, breadth and height). The width and breadth were defined by the extents of a commercial LED module (Vossloh-Schwabe WU-M-444/B-NW, Ref. No. 553927). This was chosen so any subsequent experimental analysis could employ a readily available part. Heatsink height was an arbitrary value in keeping with the base dimensions of the part. The heatsink base was a 5 mm thick plate leaving an overall fin height of 60 mm. The wall thickness of the fins was approximately 3 mm, although some small variation resulted from the way these models were defined. The heatsink models were created to allow fin spacing to be modified. Preliminary trials, using CFD analysis, were conducted to identify form which produced the lowest thermal resistance within these bounds.

Table 1. Summary of heatsink designs shown in Figure 1

Configuration	Description
Parallel plate	Conventional flat plate fins arranged in parallel fashion
Radial plate	Conventional flat plate fins arranged in radial fashion
Capped radial plate	As per "radial plate" design with a horizontal plate (cap) across the top of the fins. Open centre to cap intended to promote airflow inwards across fin surface
Spiral plate	Similar to "radial plate" but with curved fin profile to increase surface area available for heat transfer
Capped spiral plate	As per "spiral plate" design with a horizontal plate (cap) across the top of the fins. Open centre to cap intended to promote airflow inwards across fin surfaces
Diagonal plate	Similar to "parallel plate" heatsink. Fins in each quadrant oriented towards heatsink centre to avoid obstruction of fluid flow
Staggered pin	Pin fins in a hexagonal array pattern
Capped staggered pin	As per "staggered pin" design with a horizontal plate (cap) across the top of the fins. Open centre to cap intended to promote airflow inwards across fin surfaces
Staggered pin with open centre	As per "staggered pin" design with pins removed from centre of heatsink to prevent obstruction of fluid flow
Stepped staggered pin	As per "staggered pin" design with outer fin height reduced to eliminate coolest regions from heatsink
Mesh	Interwoven arrangement of channels to facilitate fluid flow through structure and increase surface area available for heat transfer
Vertical tube	Vertical array of enclosed columns to increase fluid flow through chimney effect
Helical plate	As per "radial plate" but fins follow helical path along y-direction to increase surface area available for heat transfer

Figure 1. Passive cooled heatsink designs.

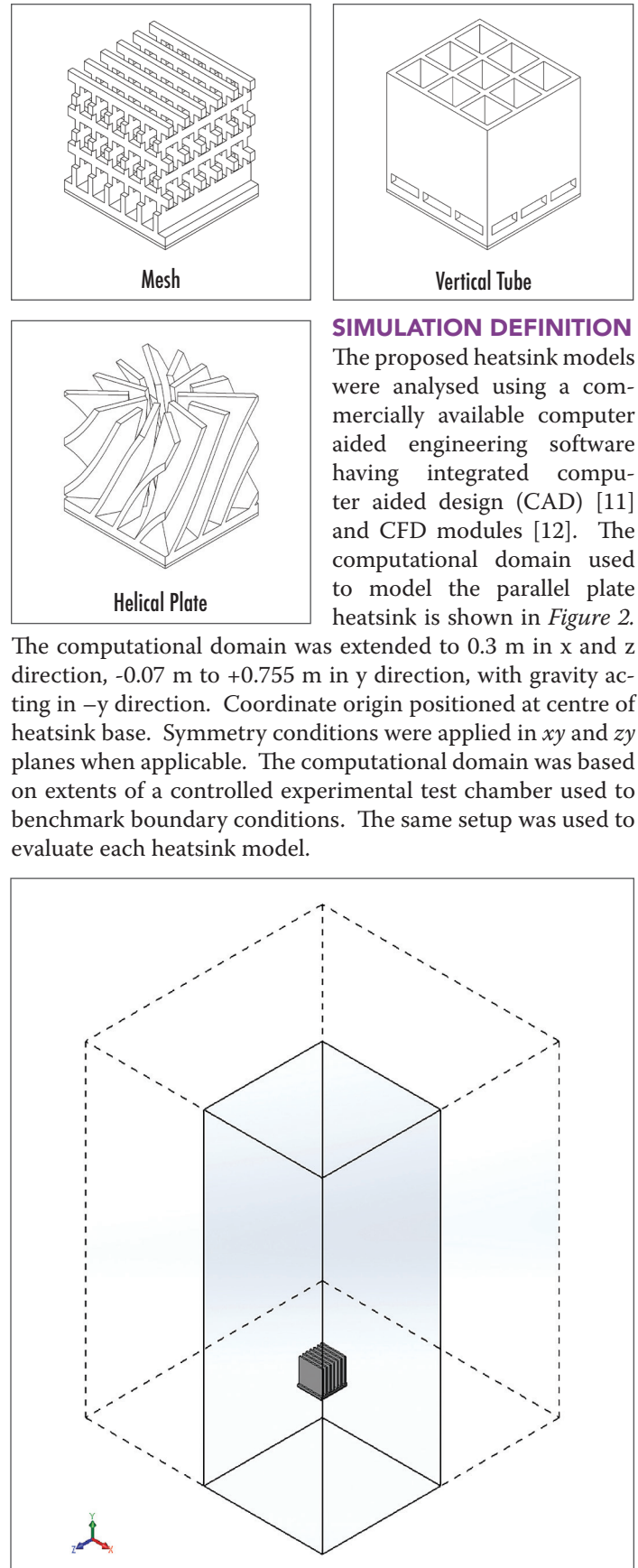
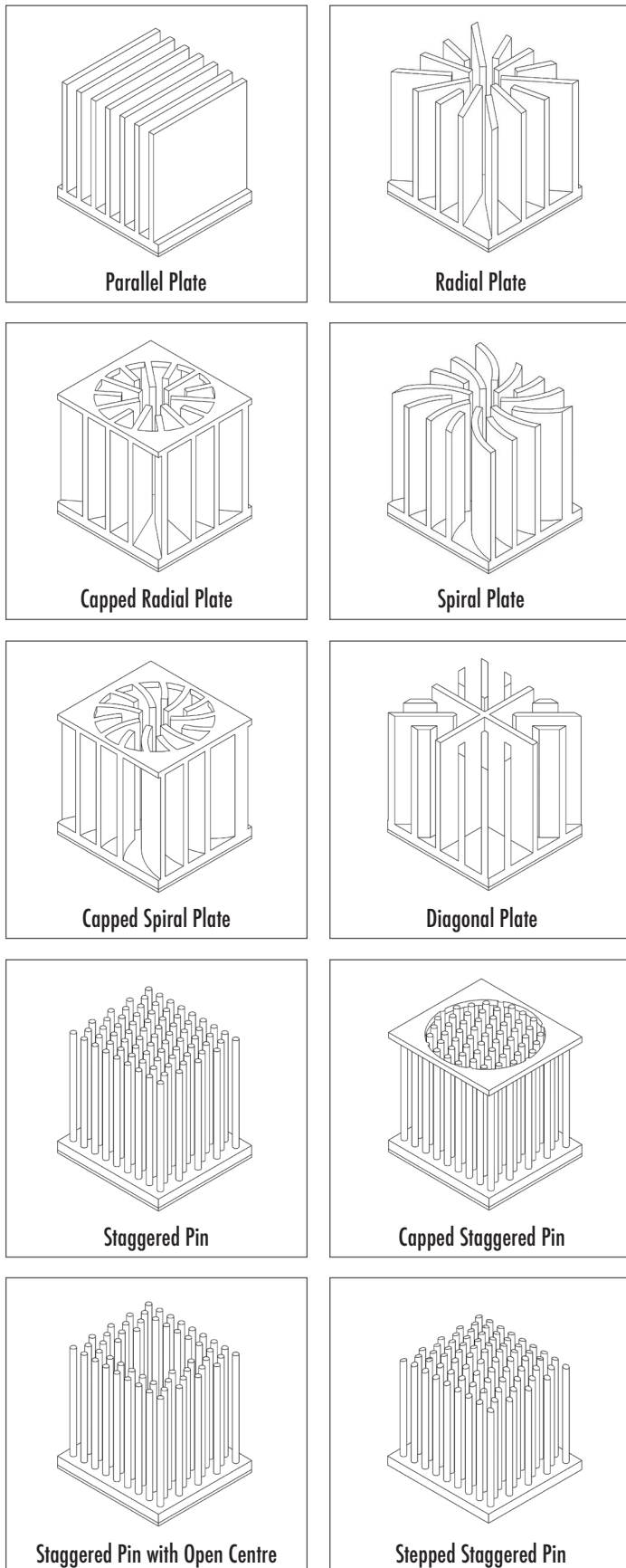


Figure 2. Heatsink computation domain.

## SIMULATION DEFINITION

The proposed heatsink models were analysed using a commercially available computer aided engineering software having integrated computer aided design (CAD) [11] and CFD modules [12]. The computational domain used to model the parallel plate heatsink is shown in Figure 2.

The computational domain was extended to 0.3 m in x and z direction, -0.07 m to +0.755 m in y direction, with gravity acting in -y direction. Coordinate origin positioned at centre of heatsink base. Symmetry conditions were applied in xy and zy planes when applicable. The computational domain was based on extents of a controlled experimental test chamber used to benchmark boundary conditions. The same setup was used to evaluate each heatsink model.

The computational mesh is shown in *Figure 3*, which is a non-conformal structured Cartesian grid. For a practical compromise between predictive accuracy and processing resources the target computational mesh employed 100,000 to 150,000 cells per quarter domain. At least five cells spanned each inter-fin space. The maximum and minimum heatsink temperatures were used as convergence goals. Convergence criteria were determined automatically by the CFD package.

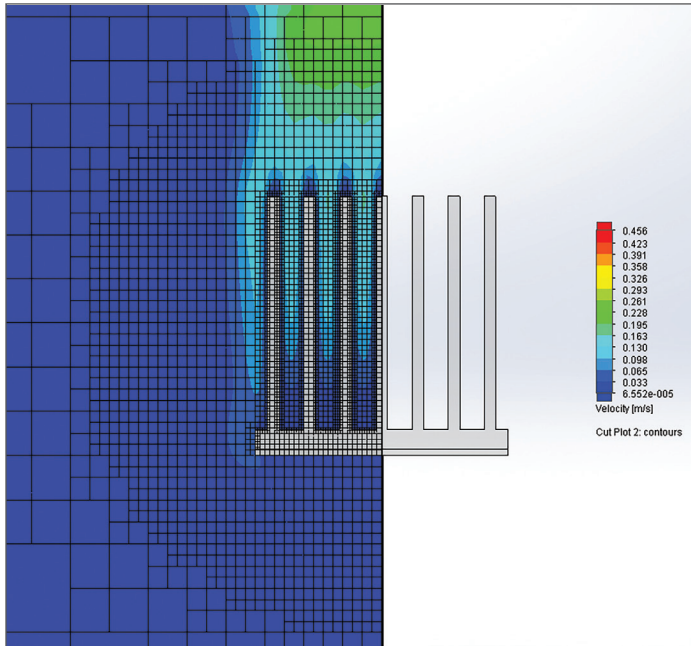


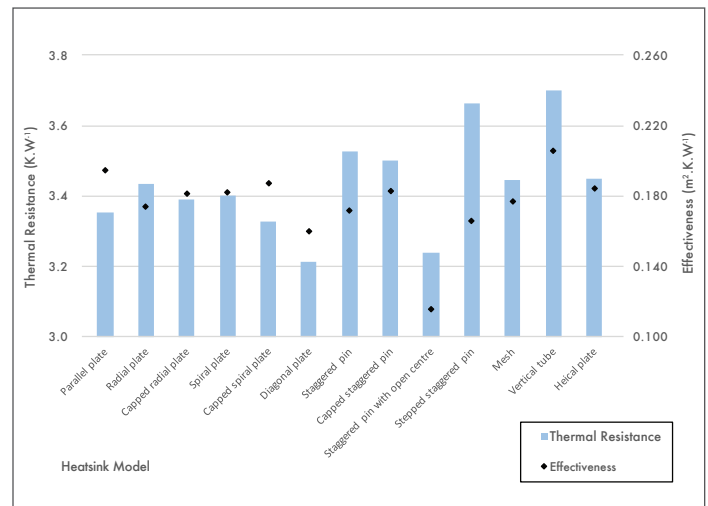
Figure 3. Local mesh refinement applied around heatsink.

The heatsink body was treated as a single homogeneous part. It was oriented with the base horizontal (parallel to  $xz$  plane). The LED module was included in the simulation model as a separate body attached to the bottom face of the heatsink. The surfaces of this body were exposed to the surrounding environment so permitted heat transfer from the subject. This was consistent across all models. Thermal interface resistance between the two bodies was defined as  $0.0001548 \text{ K.m}^2.\text{W}^{-1}$  in accordance with data supplied for an appropriate interface augmenting material [13]. The LED module comprised four LED packages mounted to an aluminium alloy substrate. As verified in a separate study [14], small features and the internal layers of the substrate (solder mask, copper trace, dielectric) can be omitted from the simulation model but thermal loads should be applied as discrete sources across each component package's footprint region for maximum confidence in the results. Each LED was assigned a thermal power of 1.5 W. Radiative heat transfer was included in the simulation but its role was not optimised. The heatsink surface was assigned an emissivity of 0.1 to represent a reflective silver finish. The low emissivity value represents an approximate "as machined" finish on the basis this would be the simplest to reproduce for future experimental validation. The LED module was assigned an emissivity of 0.8 to approximate the component's surface finish.

Computational analysis is subject to considerable uncertainty [15]. A preliminary benchmark analysis was conducted on a similar case to validate the simulation parameters employed here. The subject shared the same material properties, surface finish, mechanical configuration, operating parameters, heat source and test environment. The results were within a 5% margin for error. Absolute accuracy was not critical in this study. The objective was to evaluate the performance of different concepts. A relative estimate is sufficient to guide this process, which these simulation conditions achieve.

## RESULTS

The resulting thermal resistance and effectiveness of each heatsink model was calculated and plotted in *Figure 4*.



Note: Heatsink geometries detailed in Table 1.

Figure 4. Comparison of numerically predicted heatsink concept's thermal performance

These results were consistent with expectation. The thermal resistance of the models evaluated here ranged between  $3.21 \text{ K.W}^{-1}$  (diagonal plate) and  $3.70 \text{ K.W}^{-1}$  (vertical tube). With respect to the smallest value this is a margin of 15%. Effectiveness spanned  $0.116 \text{ m}^2.\text{K.W}^{-1}$  (staggered pin with open centre) and  $0.206 \text{ m}^2.\text{K.W}^{-1}$  (vertical tube). This represents a margin of 78% compared to the best performing. Some key points to summarise are:

- There was no apparent correlation between thermal resistance and effectiveness. Neither criteria offered a complete assessment of performance.
- The basic parallel plate heatsink model achieved a thermal resistance of  $3.35 \text{ K.W}^{-1}$  but was one of the least effective designs ( $0.195 \text{ m}^2.\text{K.W}^{-1}$ ).
- The radial plate heatsink imposed higher thermal resistance ( $3.44 \text{ K.W}^{-1}$ ) but was also more effective ( $0.174 \text{ m}^2.\text{K.W}^{-1}$ ) than the parallel plate heatsink design. This appeared to be because the arrangement of fins did not obstruct airflow from any direction but provided an overall smaller surface area restricts heat transfer.



- The spiral plate fin arrangement provided greater surface area than the radial plate heatsink. This resulted in  $0.04 \text{ K.W}^{-1}$  (1.1%) lower thermal resistance but its poor utilisation led to a  $0.008 \text{ m}^2.\text{K.W}^{-1}$  (4.6%) decrease in effectiveness.
- The diagonal plate heatsink offered the lowest thermal resistance. A number of factors appeared to contribute to this. The parallel fin arrangement maintained the optimum spacing for fluid flow, the fin positions optimised thermal conduction away from the source, and the geometry did not obstruct fluid flow from any direction.
- Excluding pins from the centre of the staggered pin heatsink appeared to enhance fluid flow whilst removing ineffective heat transfer surfaces. Consequently it provided one of the lowest thermal resistances ( $3.24 \text{ K.W}^{-1}$ ) along with the highest effectiveness ( $0.116 \text{ m}^2.\text{K.W}^{-1}$ ).
- As demonstrated by the staggered pin and stepped staggered pin design, removing the coolest portions of the heatsink showed limited benefit. Between the two models there was just  $0.006 \text{ m}^2.\text{K.W}^{-1}$  (3.5%) improvement in effectiveness but an accompanying  $0.13 \text{ K.W}^{-1}$  (3.7%) increase in thermal resistance.
- In all instances, adding a horizontal cap to the top of the heatsink reduced thermal resistance (by an average of 1.5%) but also compromised the effectiveness (4.2%) demonstrating the additional surface area was poorly utilised
- Restricted thermal transfer through the structure and poor fluid flow hinders the performance of the vertical tube and mesh heatsinks. However, these models did reveal the small buoyancy driven, passive convection forces can be used to manipulate entrained fluid flow.
- The vertical tube concept offered the worst performance by under both criteria (thermal resistance and effectiveness) so would be unattractive for further consideration.
- The helical plate heatsink was  $0.010 \text{ m}^2.\text{K.W}^{-1}$  (5.7%) less effective than straight radial fins. This appeared to be because the helical form obstructed fluid flow and due to the way it was defined reduced the fin thickness. As a result fin efficiency and performance was reduced.

## CONCLUSIONS

The primary objective of this study was to develop criteria to compare the performance of different heatsinks. The results demonstrated simple, but well defined, methods to achieve this. They were applied to various heatsink designs and those offering superior performance were revealed. This ability can be used to direct development towards better performing strategies or quantify the impact of any changes.

A conventional parallel plate fin heatsink was neither the most effective or offered lowest thermal resistance. By employing a superior design it was possible to reduce thermal resistance by  $0.14 \text{ K.W}^{-1}$  (4.2%) or improve effectiveness by  $0.079 \text{ m}^2.\text{K.W}^{-1}$  (40.5%). A pin fin heatsink with no pins at its centre was the most effective ( $0.116 \text{ m}^2.\text{K.W}^{-1}$ ) concept while a heatsink employing parallel plate fins in a diagonal arrangement provided the lowest thermal resistance ( $3.21 \text{ K.W}^{-1}$ ). Only thirteen simple heatsink models were analysed in this study. A thorough and definitive comparison of performance would demand more detailed assessment. For more complex models, incorporating multi-objective optimisation, the number of parameters to consider would quickly become impractical. In an effort to manage this a number of constraints were applied. A broader exploration of various concept's potential without the arbitrary physical constraints imposed here would be valuable. It was the author's belief that the results still provide an acceptable indication of performance and demonstrate the ability to determine which concepts offer the most potential for development.

## ACKNOWLEDGEMENTS

The Authors wish to acknowledge TamLite Lighting Ltd. for their unconditional support for, and contribution of various resources to, this investigation.

## REFERENCES

- [1] Kraus, A.D., and Bar-Cohen, A., Design and Analysis of Heat Sinks, First Edition, John Wiley and Sons, New York, USA (1995).
- [2] Bar-Cohen, A., Bahdur, R., and Iyengar, M., "Least-Energy Optimisation of Air Cooled Heat Sinks for Sustainability-Theory, Geometry and Material Selection," *Energy*, Vol. 31, No. 5, pp. 579-619 (2006).
- [3] Lassance, C. J. M., and Eggink, H. J., "A Method to Rank Heat Sinks in Practice: the Heat Sink Performance Tester," In proceedings of the 21st Annual IEEE Semiconductor Thermal Measurement and Management Symposium (Semi-therm), San Jose, CA, USA, March 15–17, 2005, pp. 141-145.
- [4] McKinsey & Company, "Lighting the way: Perspectives on the Global Lighting Market," Second Edition (2012), [https://www.mckinsey.de/files/Lighting\\_the\\_way\\_Perspectives\\_on\\_global\\_lighting\\_market\\_2012.pdf](https://www.mckinsey.de/files/Lighting_the_way_Perspectives_on_global_lighting_market_2012.pdf), accessed August 15, 2016.
- [5] Chang, M. H., Das, D., Varde, P. V., and Pecht, M., "Light Emitting Diodes Reliability Review," *Microelectronics Reliability*, Vol. 52, No. 5, pp. 762-782 (2012).
- [6] US DOE, "Life-Cycle Assessment of Energy and Environmental Impacts of LED Lighting Products. Part 1: Review of the Life-Cycle Energy Consumption of Incandescent, Compact Fluorescent, and LED lamps" (2012), [http://energy.gov/sites/prod/files/2015/10/f27/2012\\_LED\\_Lifecycle\\_Report.pdf](http://energy.gov/sites/prod/files/2015/10/f27/2012_LED_Lifecycle_Report.pdf), accessed August 14, 2016
- [7] US DOE, "Life-Cycle Assessment of Energy and Environmental Impacts of LED Lighting Products. Part 2: LED Manufacturing and Performance" (2012), <http://energy.gov/sites/>

prod/files/2015/10/f27/2012\_led\_lca-pt2\_0.pdf, accessed August 14, 2016.

[8] Sadeghi, E., Bahrami, M., and Djilali, N. "Thermal Spreading Resistance of Arbitrary-Shape Heat Sources on a Half-Space: A Unified Approach," IEEE Transactions on Components and Packaging Technologies, Vol. 33, No. 2, pp. 267-277 (2010).

[9] Poppe, A., Kolla, E., Toth, Z., and Simonovics, J., "Characterization of Heat-Sinks of Socketable LED Modules using Thermal Transient Testing," in Proceedings of the 20th International Workshop on Thermal Investigations of ICs and Systems (THERMINIC), Greenwich, London, UK, September 24-26, 2014.

[10] Farkas, G., and Poppe, A., "Thermal Testing of LEDs," Chapter 10 in: Thermal Management of LED Applications: Volume 2 - Solid State Lighting Technology and Application, Lasance C.J.M. and Poppe A. (Eds), Springer, New York, USA, pp. 73-165 (2014).

[11] Dassault Systemes, Solidworks Professional 2015 x64 Edition, SP 2.1, <http://www.solidworks.com/sw/products/3d-cad/solidworks-professional.htm>, accessed 15th August 2016.

[12] Dassault Systemes, Solidworks' Flow Simulation 2015

SP2.0. Build: 2990, <http://www.solidworks.com/sw/products/simulation/flow-simulation.htm>, accessed August 15, 2015.

[13] HALA CONTEC Graphite Foil TFO-S-CB, available at: [http://www.hala-tec.de/fileadmin/user\\_upload/datenblaetter-en/E\\_HALA\\_TFO-S-CB.pdf](http://www.hala-tec.de/fileadmin/user_upload/datenblaetter-en/E_HALA_TFO-S-CB.pdf), accessed August 15, 2016.

[14] Pryde, J., Whalley, D., and Malalasekera, W., "An Assessment of Computational Fluid Dynamic Simulations and Appropriate Simplifications used for the Development of LED Luminaires," in Proceedings of the 20th International Workshop on Thermal Investigations of ICs and Systems (THERMINIC), Greenwich, London, UK, September 24-26, 2014.

[15] Lasance, C.J.M., "The Conceivable Accuracy of Experimental and Numerical Thermal Analysis of Electronic Systems," IEEE Transactions on Components and Packaging Technologies, Vol. 25, No. 3, pp. 366-382 (2002).

## CONTACT INFORMATION

**James Pryde**

Loughborough University  
Loughborough, LE11 3TU, UK

Email: [j.r.pryde@lboro.ac.uk](mailto:j.r.pryde@lboro.ac.uk)

# Full Lineup of Speed Control Fans



## Engineered to Perform, Built to Last

### Pulse Width Modulation (PWM) Speed Control Technology

PWM regulates the voltage signal between fully on and fully off to control the speed of the fan. The main advantages are:

- Flexible Speed Control
- Low Switching Noise
- Low Vibration
- High Power Efficiency

web: [www.delta-fan.com/pwm](http://www.delta-fan.com/pwm) | email: [dcfansales.us@deltaww.com](mailto:dcfansales.us@deltaww.com) | tel: 866-407-4278







# Cooling Matters.

Find your thermal solutions here.

- Read the latest news, standards & product updates
- Find products & services with our Buyers' Guide
- Download the most recent issue of Electronics Cooling
- Share and comment on stories with colleagues

**Electronics**  
**COOLING**

[electronics-cooling.com](http://electronics-cooling.com)



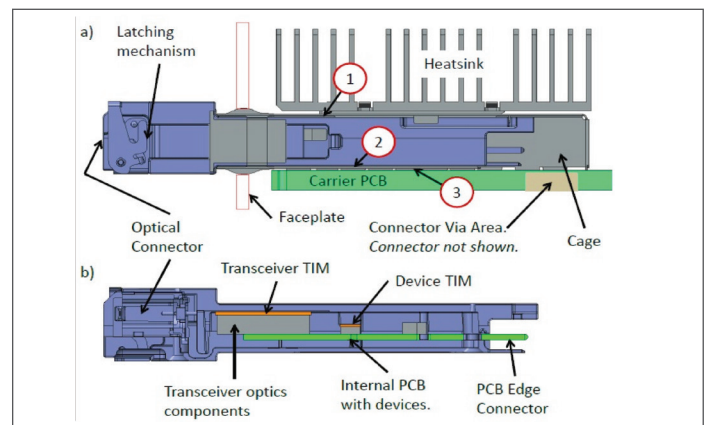
# Pluggable Optics Modules - Thermal Specifications: Part 2

Terence Graham and Bonnie Mack,  
Ciena Corporation

## INTRODUCTION

In Part 1 of this article [1] the overall thermal environment for pluggable optical modules (POMs) was described, with the effect of both out of flatness and source locations relative to heatsink contact area also examined. The article also introduced the relevant sections of the multi-source agreements (MSAs) [2-5] and optical internetworking forum (OIF) thermal interface specifications [6]. In this article (Part 2), the results are extended to examine the effects of heat sources on the carrier printed circuit board (PCB) and their relation to the calibration of internal temperature sensors of a C-form-factor-pluggable 2 (CFP2) transceiver model with a generic zinc-alloy-case. This was done by exploring the heat exchange between it and both the carrier PCB and heatsink.

This article delves further into the influence of the thermal interface location and its size relative to the internal PCB heat source location on the cooling of another form factor, Quad Small Form-factor Pluggable (QSFP). The QSFP is a common POM that presently has the highest power density of all the form factors [7]. The complete QSFP and cage assembly is shown in *Figure 1* and described further in [1,8]. CFP2 POM and cage are similar but larger.



*Note: Numbered narrow air gap locations; (1) module to top of cage, (2) module to bottom of cage, (3) bottom of cage to carrier PCB, and (4) sides of module to sides of cage (not shown).*

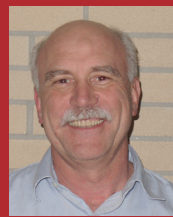
**Figure 1. Pluggable optics module (POM): a) QSFP in cage section at inside edge of cage, b) QSFP section showing typical internal layout.**

The numerical analysis presented in this article was undertaken using commercially available computation fluid dynamics



**BONNIE  
MACK**

has been working in electronics cooling for over 25 years. She has worked at Nortel, Solectron and as an independent contractor. She is currently a senior thermal engineer at Ciena specializing in thermal simulation and testing. She is a past chair of the Semi-Therm conference and currently serves on the program committee. She is a past member of the Harvey Rosten Award for Excellence selection committee. She received a B.A.Sc. and a M.A.Sc. in engineering at the University of Waterloo.



**TERENCE  
GRAHAM**

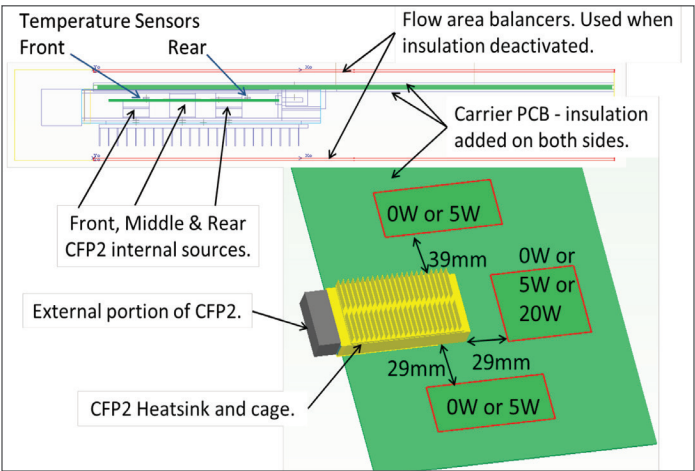
received his B.Sc. degree in Mathematics and Engineering from Queen's University, and his M.A.Sc. and Ph.D. in Aerospace Studies from University of Toronto. He has 15 years of experience in electronics cooling system design and development for optical networks and concentrating solar photovoltaic systems. He is currently a senior thermal engineer at Ciena who is active in the Optical Interconnecting Forum. Previously he worked with Nortel, Atomic Energy of Canada, and University of Toronto. He has more than 20 articles in archival journals and conference proceedings in the areas of air cushion technology, sealing technology, ice slurry equipment, and in thermal design and development for optical telecommunications systems.

(CFD) software, with complete modelling details provided in [8]. Key modeling aspects are discussed here. Air thermophysical properties were modelled at 50 °C and 1800 m elevation conditions. These are operating temperature limits for telecommunication equipment from GR-63-Core [9]. For the CFP2 and QSFP modules the upstream air flow velocity was set at 2 m/s and 1.5 m/s, respectively. These cooling air flow speeds lie within the typical range for POM environments. Other analysis variables are summarized in the appropriate section.

No experimental results are presently available for the configurations studied here, but measurements on commercial product PCBs with thermal mock-up POMs that used the same modelling techniques and software have shown good design level accuracy to predicted temperatures, and to trends in internal sensor calibration as a result of PCB heating. On this basis, confidence is established on the accuracy of the numerical predictions presented in this article.

CALIBRATION OF NUMERICAL WIND TUNNEL GEOMETRY FOR CFP2 HEAT-FLOW ANALYSIS

The wind tunnel geometry, location of the carrier PCB heat sources, and temperature sensors are shown in Figure 2. Three carrier PCB heating layouts are used to simulate local processors or other power dissipating components and are summarized in Table 1. The geometry of the CFP2 modeled in [1] was updated with more detail for the heat sources and their connection to its lid and base. The internal power dissipation of CFP2 was reduced from 12 W to 9 W, so as put its operation into power density class 4 (pd04) [7]. In this case the thermal interface contact area is modelled as perfectly flat (0 mm) with 0.119 °C/W thermal resistance representing 15 N contact force and 1.6 µm Ra finish per the MSA specification [2]. The test case variables for CFP2 heat-flow analysis are summarized in Table 1.



Note: Front and rear sensors monitor the internal PCB temperature.  
Figure 2: Numerical wind tunnel geometry for CFP2 heat-flow analysis [8].

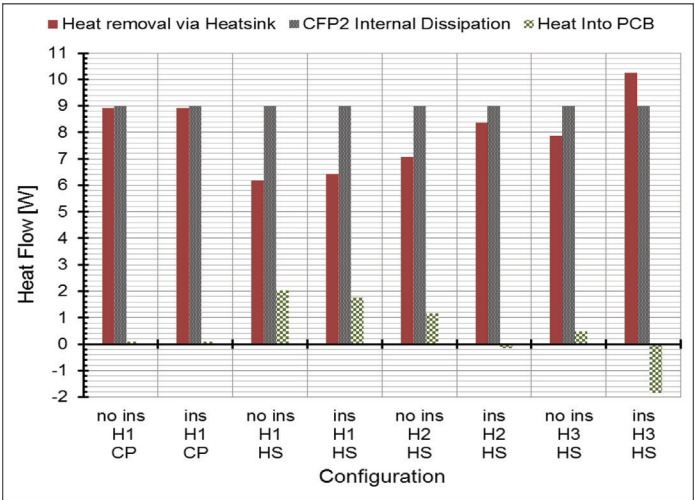
Thermal insulation was added to the carrier PCB, Figure 2, to evaluate its effectiveness in controlling heat flow when calibrating

the internal front and rear temperature sensors. The CFP2 was also modelled with a cold plate (isothermal heatsink) in a natural convection environment. This was recommended in [7] for measuring the thermal interface contact resistance and for use in calibrating internal temperature sensors. In the insulation studies, 1 mm of insulation having a thermal resistance equivalent to approximately 2 mm of quiescent air, or 10 mm of dry wood, was applied to both sides of the carrier PCB to enforce heat removal via the heatsink, or cold-plate, rather than directly to the air.

Table 1. Numerical modelling test case matrix for CFP2 heat-flow analysis.					
Carrier PCB Heating Layouts		Cold Plate Natural Convection		Heat Sink 2 m/s airspeed upstream	
		Not Insulated	Insulated	Not Insulated	Insulated
H1	0 W total (calibration configuration)	Yes	Yes	Yes	Yes
H2	15 W total with 3 x 5 W heat sources	No	No	Yes	Yes
H3	30 W total with 2 x 5 W side-sources and a 20 W source near the connector	No	No	Yes	Yes

Note: CFP2 module total heat dissipation = 9 W, carrier PCB heating layouts shown in figure 2.

POMs usually have internal sensors that can monitor the module operating temperatures and are calibrated across the product specified operating temperature range. The front and rear sensor locations in the POM, Figure 2, are representative locations for such sensors. The CFP2 model has two sensors on the secondary side of the internal PCB. One is centered under the two front heat sources. The other is centered just behind the two rear heat sources. Details of the internal design parameters of the CFP2 are en in [8].



Note: Positive heat flow is out of module, CP = Cold Plate, HS = Heatsink, ins = insulated, and no ins = uninsulated.  
Figure 3: Numerically predicted heat flow paths from CFP2 module.

Figure 3 shows the predicted heat flows from the CFP2 module to both its heatsink and the carrier PCB for several insulation and PCB heat dissipation conditions. It shows that for carrier PCB heating layouts H1, a cold plate and natural convection environment, over 99% of the CFP2 dissipation is removed across the thermal interface area. In contrast, with a heatsink instead of a cold plate attached, less than 72% of the heat is removed through the heatsink, even with an insulated carrier PCB. The results for carrier PCB heating layouts H2 and H3 show significant conduction from the carrier PCB into the POM when the PCB is insulated.

The nominal thermal resistance for the CFP2-heatsink interface area,  $r_{Int}$ , is defined as in [7]:

$$r_{Int} = \Delta T_{MP-HS} / (P_{CFP2} / A_{Int}) \text{ [m}^2\text{°C / W]}$$

where:

$T_{MP}$  = Temperature at CFP2 lid "Hot Spot" monitor point [°C],  
 $A_{Int}$  = Thermal interface area [m<sup>2</sup>],  $P_{CFP2}$  = CFP2 power dissipation [W],

$\Delta T_{MP-HS}$  = Temperature difference between the CFP2 lid "Hot Spot" ( $T_{MP}$ ) and center of heatsink contact pad [°C]

As defined,  $r_{Int}$  includes the effects of heat spreading in both the CFP2 lid and heatsink base. Figure 4 compares  $T_{MP}$  to temperatures differences with the front and rear sensor locations. In the current model, the difference between  $T_{MP}$  and the front-sensor-temperature,  $\Delta T_{MP-Front\ Sensor}$ , remain relatively constant, i.e. less than 0.4°C, over the thermal environments modelled while  $\Delta T_{MP-rear\ sensor}$  varies by more than 4.5°C. Consequently the front temperature sensor would be the better choice to calibrate to represent the monitor point since its dependence on heat conducted from the carrier PCB is minimal. The variation in the rear sensor temperature is more than the typical accuracy specification of  $\pm 3^\circ\text{C}$ . Therefore, the cold plate method would be the most repeatable for calibration.

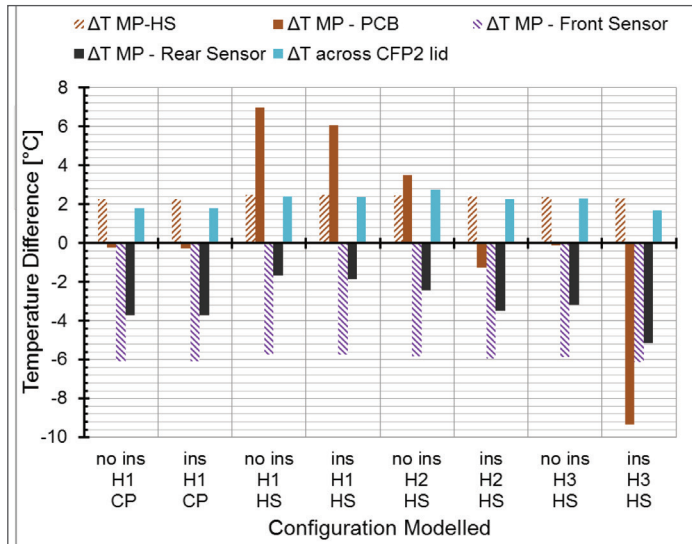


Figure 4: Numerically predicted temperature difference between CFP2 lid "Hot Spot" and front and rear temperature sensor locations.

Using a cold plate, the predicted thermal resistance should be reasonably accurate since over the majority of the heat flows through the heat sink thermal interface area ( $A_{Int}$ ), and cold plate base, will be uniform by design. With a cold plate,  $r_{Int}$  is twice the nominal applied contact resistance of  $3.2^\circ\text{C}\cdot\text{cm}^2/\text{W}$ . Spreading effects in the CFP2 lid accounts for this added resistance even with good distribution of the heat sources.  $\Delta T_{MP-HS}$  remains greater than the  $2^\circ\text{C}$  specification [7] for high performance interfaces. Even assuming perfect flatness, the MSA maximum of  $1.6\ \mu\text{m Ra}$  surface finish is clearly not sufficient for the 9W dissipation of this CFP2 POM for a high temperature ambient.

## QSFP MODEL – EXPANDING ON THE EFFECT OF SPREADING RESISTANCE

The majority of QSFP heat is dissipated close to the faceplate and not directly underneath the heatsink contact area. A numerical wind tunnel study was conducted to explore the internal thermal resistances and develop methods of reducing the QSFP temperatures. The numerical model shown in Figure 5 is detailed in [8] and is similar to that of [10] having a 5 W QSFP and a power density of  $1.34\ \text{W}/\text{cm}^2$ , class pd14 [7]. Cooling was via a typical aluminum off-the-shelf heatsink. The model was used to predict the effect of changes in the heat source locations relative to the nominal heatsink contact area, i.e. the thermal interface area of reference [7], is shown Figure 5. For scenario (d) the 5 mm extension of the heatsink contact area towards the transceivers, the power density decreases to  $1.14\ \text{W}/\text{cm}^2$  or to class pd12 [7].

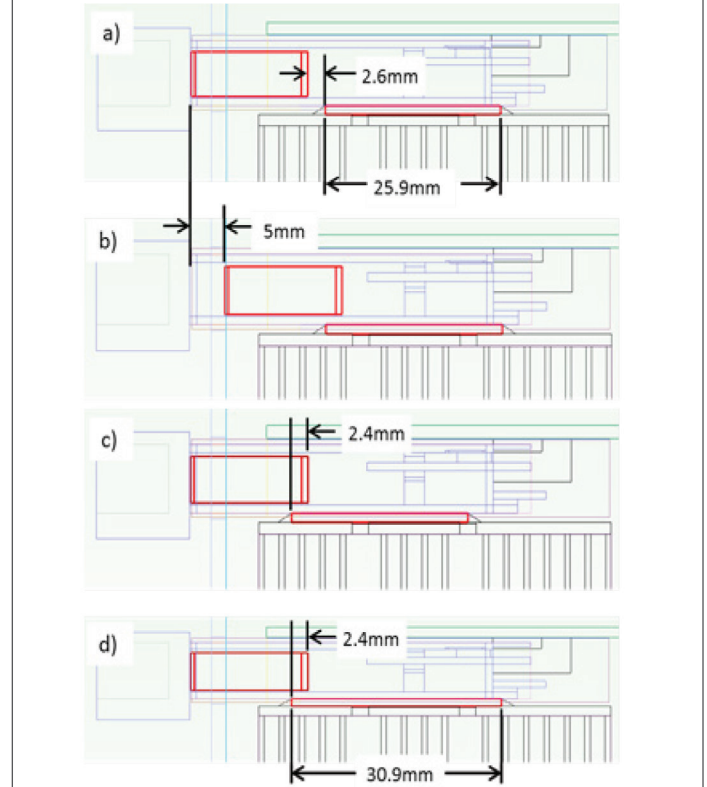


Figure 5: Modelling scenarios for the QSFP: (a) Original, (b) Transceivers 5 mm closer to heatsink contact, (c) Heatsink contact 5 mm closer to transceivers, and (d) Heatsink contact 5 mm longer towards transceivers.

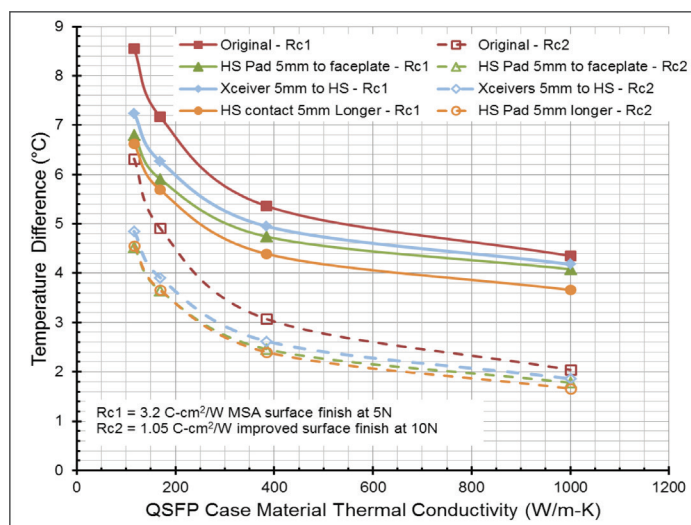


As with the CFP2, contact resistance with the heatsink was estimated per the method of [11] for a perfect flatness at two different surface roughness and load conditions:  $R_{c1}$  for 1.6  $\mu\text{m}$  Ra and 5 N contact force, and  $R_{c2}$  for 0.6  $\mu\text{m}$  Ra finish and 10 N contact force. Results were calculated for QSFP case material thermal conductivities of 116, 169, 385 and 1000 W/m-K corresponding to a zinc alloy, high grade aluminum casting, copper and an ultra-high conductivity material respectively.

The temperature difference results shown in Figure 6 illustrate the importance of the surface finish of the case (controlled by POM design) and heatsink (controlled by system design), and of locating the heat sources and the thermal interface area as closely together as possible. QSFP MSA cage dimensions [4, 5] allow an increase in heatsink contact length by up to 5 mm. In the current model this larger contact resulted in a temperature decrease of more than 1.5 °C with zinc alloy case and  $R_{c1}$ . If the case material conductivity is increased to 169 W/m-K or 385 W/m-K, further decreases of 1 °C to 2 °C, respectively, could be achieved (solid orange line). While very high case conductivity representing an exotic material was examined, changing QSFP case material to copper from zinc alloy can improve performance by 1.5 °C to 3 °C for MSA heatsink contact design (solid red line).

Decreasing the contact resistance to  $R_{c2}$  would bring total improvement to approximately 5 °C (solid red zinc alloy to dashed red copper). These are significant when the overall ambient to case temperature budget could be 15 °C or less for downstream components in a Telcordia environment [12].

Even with these potential gains the high power density of the QSFP means it is unlikely that the OIF high performance interface specification of 2 °C between the monitor point and the heatsink will be attained for plug dissipation greater than 4.2 W.



Note: Thermal contact resistance:  $R_{c1}$  = 1.6  $\mu\text{m}$  Ra and 5 N loading, and  $R_{c2}$  = 0.6  $\mu\text{m}$  Ra and 10 N loading.

Figure 6: Numerically predicted temperature difference between QSFP lid hot spot monitor point and heatsink base.

## DISCUSSION

The OIF agreement [7] specifies information required by system designers for preliminary, simplified system, and detailed system analyses. Simple estimations of the temperature loss to the heatsink are feasible by defining power density classes and requiring a measurement of the overall thermal resistance between the monitoring point on the POM module lid and the heatsink. This measurement is to be done on a module in its cage, and powered from an insulated carrier PCB with a cold plate heatsink to ensure the thermal interface resistance measurement includes the POM's contribution to the interface resistance. For this environment, the results presented here show that 99% of the CFP2 dissipation flows through the interface of interest, whereas other test methods have net heat transfer from the POM to the carrier PCB, or to the POM from the carrier PCB.

Final POM module thermal assessment is at present only available with a computationally expensive detailed model created from the information specified in [7] and either built by the system designer with information from the module supplier, or is a model supplied by the module vendor, likely under some form of non-disclosure agreement (NDA). An alternative to this approach has not yet been explored is the development of a Delphi-type resistance network [13]. A model of this type could be used to model the connections to the carrier PCB, surrounding air and heatsink with distributed internal heat sources similar to a multi-junction integrated circuit device. This could be provided by POM module vendors without giving internal details of the module.

## SUMMARY

Thermal interface resistance of pluggable optical modules (POMs) is affected by design factors under the control of both the system and module designers. In particular, surface finish and flatness have a strong influence within normally accepted manufacturing and machining practices.

POM designers can reduce thermal spreading losses by keeping the heat sources close to the thermal interface area and by increasing the thermal conductivity of the case materials. For Quad Small Form-factor Pluggables (QSFPs), the size of the cage hole for heatsink contact given in the multi-source agreement (MSA) can be increased giving a reduction in the thermal interface resistance and therefore module temperature.

The Optical Internetworking Forum (OIF) definition of thermal interface gives a useful division of the responsibilities for module cooling at the module case. The thermal interface resistance is defined for an ideal heatsink contact on the system side so that POM designers can optimize module surface contact and spreading thermal resistance.

Figures 3 and 4 highlighted the importance of the heat paths between the POM and the carrier printed circuit board (PCB).

In the absence of junction-to-board thermal resistance ( $R_{j-b}$ ) type information, thermal assessments are biased towards lid-only cooling. Real applications include the effects of the carrier PCB. Optical module designers should therefore consider a thermal resistance network model of their optical plugs to complement the thermal interface information defined in the OIF Implementation Agreement (IA).

## REFERENCES

- [1] Mack, B., and Graham, T., "Pluggable Optics Module – Thermal Specifications, Part 1," Electronics Cooling, June 2016, <http://www.electronics-cooling.com/2016/07/pluggable-optics-modules-thermal-specifications-part-1/>, accessed August 13, 2016.
- [2] Hiramoto, K., "CFP MSA CFP2 Hardware Specification," Revision 1.0, July 2013, [http://www.cfp-msa.org/Documents/CFP2\\_HW-Spec-rev1.0.pdf](http://www.cfp-msa.org/Documents/CFP2_HW-Spec-rev1.0.pdf), accessed August 13, 2016.
- [3] Oomori, H. Hardware Technical Editor, CFP MSA CFP4 Hardware Specification, Revision 1.0, August, 2014, [http://www.cfp-msa.org/Documents/CFP-MSA\\_CFP4\\_HW-Spec-rev1.0.pdf](http://www.cfp-msa.org/Documents/CFP-MSA_CFP4_HW-Spec-rev1.0.pdf), accessed August 13, 2016.
- [4] SFF Committee, "SFF-8663 Specification for QSFP+ 28 Gb/s Cage (Style A)," Revision 1.5, April 2014, <ftp://ftp.seagate.com/sff>, accessed August 13, 2016.
- [5] SFF Committee, "SFF-8661 Specification for QSFP+ 28 Gb/s 4x Pluggable Module," Revision 2.0, February 2014, <ftp://ftp.seagate.com/sff>, accessed August 13, 2016.
- [6] Optical Internetworking Forum, [www.oiforum.com](http://www.oiforum.com), accessed August 13, 2016.
- [7] IA# OIF-Thermal-01.0, "Implementation Agreement for Thermal Interface Specification for Pluggable Optics Modules," Optical Internetworking Forum, May 2015, [http://www.oiforum.com/wp-content/uploads/OIF-Thermal-01.0\\_IA.pdf](http://www.oiforum.com/wp-content/uploads/OIF-Thermal-01.0_IA.pdf), accessed August 13, 2016.
- [8] Mack, B., Graham, T., "Thermal Specifications for Pluggable Optics Modules," in 32nd Thermal Measurement, Modeling & Management Symposium (SEMI-THERM), San Jose, CA, USA, March 14-17, 2016, pp. 133-142.
- [9] Telcordia, NEBS Requirements: Physical Protection, Telcordia Technologies Generic Requirements, GR-63-CORE, Issue 3, March 2006.
- [10] OIF-PLUG-Thermal-01.0, "Thermal Management at the Faceplate White Paper," Optical Internetworking Forum, March 2012.
- [11] Yovanovitch, M.M., Culham, J.R., and Teerstra, P., "Calculating Interface Resistance," ElectronicsCooling, May 1997, <http://www.electronics-cooling.com/1997/05/calculating-interface-resistance/>, accessed August 13, 2016.
- [12] TelcordiaTechnologies Generic Requirements, Generic Requirements for Telecommunications Data Center Equipment and Spaces, GR-3160-CORE, Issue 2, July 2013, [http://telecom-info.telcordia.com/ido/AUX/GR\\_3160\\_TOC.i02.pdf](http://telecom-info.telcordia.com/ido/AUX/GR_3160_TOC.i02.pdf), accessed August 13, 2016.
- [13] Lasance, C.J.M "Ten Years of Boundary-Condition Independent Compact Thermal Modeling of Electronic Parts: A Review," Heat Transfer Engineering, Vol. 29, Issue 2, pp. 149 - 168 (2008).

## CONTACT INFORMATION

**Terence Graham, Bonnie Mack**

Ciena Corporation

3500 Carling Ave.

Ottawa, Ontario, Canada

**Email:** [tgraham@ciena.com](mailto:tgraham@ciena.com); [bmack@ciena.com](mailto:bmack@ciena.com)

**DISCOVER BETTER DESIGNS, FASTER.**

FULL DETAIL  
COMPLETE PHYSICS  
EXPLORE ALL DESIGN POSSIBILITIES

info@cd-adapco.com  
cd-adapco.com

**CD-adapco**  
A Siemens Business

STAR-CCM+

# Design Considerations When Using Heat Pipes

George Meyer  
Celsia Inc.

## INTRODUCTION

This article is intended to offer design guidance when using heat pipes for the most prevalent types of electronics applications: mobile to embedded computing and server type applications with power dissipation ranging from 15 W to 150 W using processor die sizes between 10 mm and 30 mm square. Discussion is constrained to those conditions as guidelines provided may not necessarily apply for power electronics applications. In addition, discussion is focused on the most ubiquitous type of heat pipe, *i.e.* copper tube with sintered copper wick using water as the working fluid. The article is also not intended to provide detailed analysis on the proper design of heat pipes and heat sinks, but rather to offer guidance on the number and size of heat pipes used as well as to provide guidance for estimating heat sink size and determining attachment methods of the heat sink to the Printed Circuit Board (PCB). As this article does not review the fundamentals of heat pipe operation, for those readers not familiar with this technology good overviews can be found in [1-4].

As assistance, *Figure 1* serves to provide an overview of heat pipe construction and its principle of operation. A wick structure (sintered powder) is applied to the inside walls of the pipe. Liquid (usually water) is added to the device and vacuum sealed at which point the wick distributes the liquid throughout the device. As heat is applied to the evaporator area, liquid turns to vapor and moves to an area of lower

pressure where it cools and returns to liquid form. Capillary action then redistributes it back to the evaporator section.

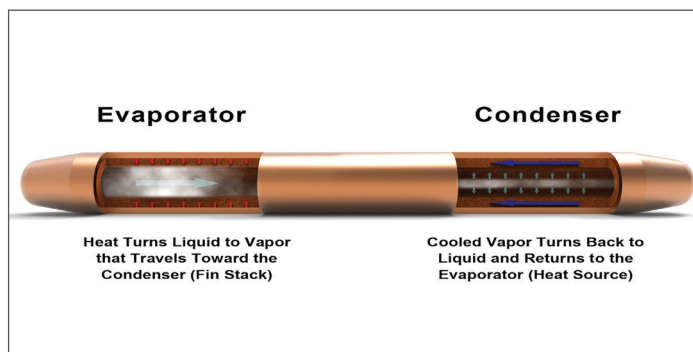


Figure 1. Heat pipe construction and principle of operation.

The application of heat pipes should be considered when the thermal design is either conduction limited or when non-thermal goals such as weight cannot be achieved with other materials such as solid aluminum and/or copper. The following factors need to be considered when designing heat pipes into a thermal solution:

- Effective thermal conductivity
- Internal structure
- Physical characteristics
- Heat sink

and are discussed in the following sections.



GEORGE  
MEYER

is a thermal industry veteran with over three decades of experience in electronics thermal management. He currently serves as the CEO of Celsia Inc., a design and manufacturing company specializing in custom heat sink assemblies using heat pipes and vapor chambers. Previously, Mr. Meyer spent twenty-eight years with Thermacore in various executive roles including Chairman of the company's Taiwan operations. He holds over 70 patents in heat sink and heat pipe technologies and serves as a chairperson for both Semi-Therm and IMAPS thermal conferences in the San Francisco area.



## 1.0 EFFECTIVE THERMAL CONDUCTIVITY

Regularly published data for heat pipe thermal conductivity typically ranges from 10,000 to 100,000 W/m.K [4]. That is 250 to 500 times the thermal conductivity of solid copper and aluminum, respectively. However don't rely on those figures for typical electronics applications. Unlike solid metal, the effective thermal conductivity of copper heat pipes varies tremendously with heat pipe length, and to a lesser degree with other factors such as the size of the evaporator and condenser as well as the amount of power being transported.

Figure 2 illustrates the effect of length on heat pipe effective thermal conductivity. In this example, three heat pipes are used to transport heat from a 75 W power source. While thermal conductivity of 10,000 W/m.K is achieved at just under 100 mm heat pipe length, a 200 mm length has less than one-third the typically published maximum thermal conductivity of 100,000 W/m.K. As observed in the calculation for effective thermal conductivity in Equation (1), the heat pipe effective length is a function of adiabatic, evaporator and condenser lengths:

$$K_{\text{eff}} = Q L_{\text{eff}} / (A \Delta T) \quad (1)$$

where:

$K_{\text{eff}}$  = Effective thermal conductivity [W/m.K]

$Q$  = Power transported [W]

$L_{\text{eff}}$  = Effective length =  $(L_{\text{evaporator}} + L_{\text{condenser}})/2 + L_{\text{adiabatic}}$  [m]

$A$  = Cross-sectional area [m<sup>2</sup>]

$\Delta T$  = Temperature difference between evaporator and condenser sections [°C]

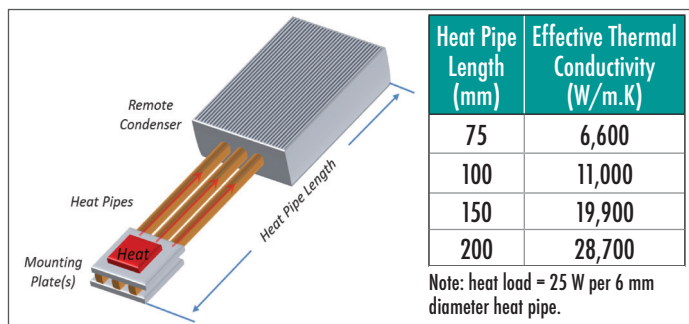


Figure 2. Measured heat pipe effective thermal conductivity as function of length.

## 2.0 INTERNAL STRUCTURE

Vendor specified heat pipe performance data are usually adequate for standard applications, but can be limited for specialized usage. Even when limiting the current discussion to copper/water/sintered wick versions, heat pipe customization can markedly affect operational and performance characteristics.

Changes to the internal structure of the heat pipe, most notably wick porosity and thickness, allow heat pipes to be tuned to meet specific operating parameters and performance characteristics. For instance, when a given diameter heat pipe is required to operate at higher power loads or against gravity, the capillary pressure in the wick needs to increase. For higher power han-

ding capacities ( $Q_{\text{max}}$ ), this means a larger pore radius. For effectively working against gravity (condenser below evaporator), this means a smaller pore radius and/or increased wick thickness. Additionally, it is possible to vary both wick thickness and porosity along the length of a single tube. Suppliers who specialize in heat pipe customization will regularly use custom formulated copper powders and/or unique mandrels to ensure the final product meets applications requirements.

## 3.0 PHYSICAL CHARACTERISTICS

With heat pipes, size generally matters most. However, changes to outward design will degrade performance for any given heat pipe, i.e. flattening and bending, in addition to the influence of gravity.

### 3.1 FLATTENING

Table 1 shows the  $Q_{\text{max}}$  for the most common heat pipe sizes as a function of diameter. As noted earlier,  $Q_{\text{max}}$  may vary amongst vendors for standard heat pipes. Therefore, in order to provide like-by-like comparison between the data presented in Table 1 it is taken from a project in which the author was involved.

Table 1. Heat pipe maximum power handing capacities as function of diameter.					
Assessment Parameter	Diameter (mm)				
	3	4	5	6	8**
Maximum power handing capacity ( $Q_{\text{max}}$ )* [Watts]	15.0	22.0	30.0	38.0	63
Typical flattening height [mm]	2.0	2.0	2.0	2.0	2.5
Resulting width [mm]	3.57	5.14	6.71	8.28	11.14
Flattened maximum power* [Watts]	10.5	18.0	25.5	33.0	52.0

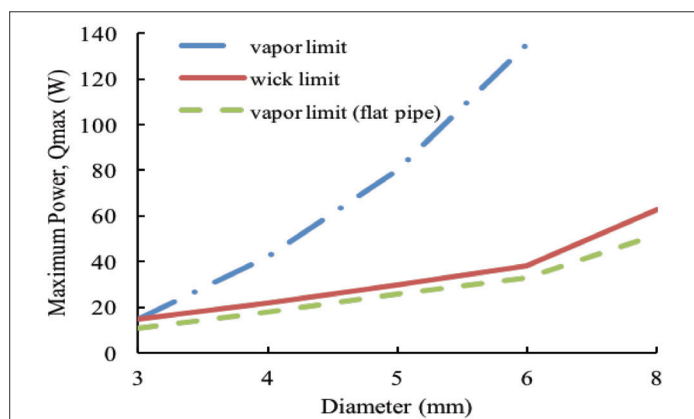
Note: \*Horizontal Operation, \*\*A thicker wick is used compared to the 3 mm to 6 mm heat pipes.

Typically, sintered copper heat pipes can be flattened to a maximum of between 30% to 60% of their original diameter. Some may argue that it is the lower figure that is more realistic, before the centerline starts to collapse, but it's really a function of technique. For example, one-piece vapor chambers which begin life as a very large heat pipe can be flattened down to 90%. In this regard, the author would like to provide a rule of thumb for how much performance will degrade for every 10% decrease in thickness, but it would be irresponsible. Why? The answer comes down to how much excess vapor space is available before the heat pipe is flattened.

Simply put, there are two performance limits important for terrestrial heat pipe applications: the wick limit and the vapor limit. The wick limit is the ability of the wick to transport water from the condenser back to the evaporator. As mentioned, the porosity and thickness of the wick can be tuned to specific applications, allowing for changes to  $Q_{\text{max}}$  and/or ability to work against gravity. The vapor limit for a particular application is

driven by how much space is available for the vapor to move from the evaporator to the condenser.

The wick (red) and vapor (blue) lines in Figure 3 plot the respective limits for the various heat pipe sizes shown in Table 1. It's the lesser of these two limits that determine  $Q_{\max}$  and as shown the vapor limit is above the wick limit, albeit only slightly for the 3 mm heat pipe. As heat pipes are flattened, the cross sectional area available for vapor to move is gradually reduced, effectively moving the vapor limit down. So long as the vapor limit is above the wick limit,  $Q_{\max}$  remains unchanged. In this example, we've chosen to flatten the heat pipes to the specifications in Table 1. As seen by the flat pipe vapor limit (green dashed line) in Figure 3, the vapor limit is below the wick limit, reducing the  $Q_{\max}$ . Flattening the 3 mm by only 33% causes the vapor limit to become the determining factor whereas the 8 mm pipe needed to be flattened by over 60% for this to happen.



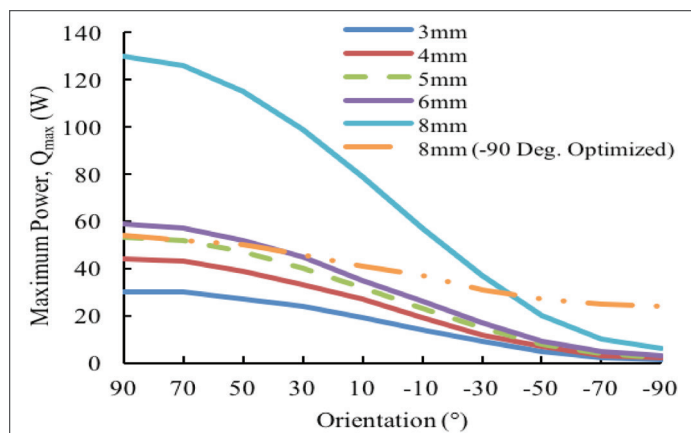
Note: Unless otherwise indicated heat pipe diameter is circular.  
Figure 3. Measured heat pipe performance limits as a function of geometry, wick and vapor limits.

### 3.2 BENDING

Bending the heat pipe will also affect the maximum power handling capacity, for which the following rules of thumb should be kept in mind. First, minimum bend radius is three times the diameter of the heat pipe. Second, every 45 degree bend will reduce  $Q_{\max}$  by about 2.5%. From Table 1, an 8 mm heat pipe, when flattened to 2.5mm, has a  $Q_{\max}$  of 52 W. Bending it 90 degrees would result in a further 5% reduction. The new  $Q_{\max}$  would be  $52 - 2.55 = 49.45$  W. Further information on the influence of bending on heat pipe performance is given in [5].

### 3.3 WORKING AGAINST GRAVITY

Figure 4 illustrates how the relative position of evaporator to condenser can affect both  $Q_{\max}$  and heat pipe selection. In each case,  $Q_{\max}$  is reduced by approximately 95% from one orientation extreme to the next. In situations where the condenser must be placed below the evaporator, a sintered material is used to allow for smaller pore radius and/or increase the wick thickness. For instance, if an 8 mm heat pipe is optimized for use against gravity (-90°), its  $Q_{\max}$  can be increased from 6 W to 25 W.



Note: Evaporator above condenser = -90°

Figure 4. Measured effect of circular heat pipe performance as function of orientation and diameter.

## 4.0 HEAT PIPE SELECTION

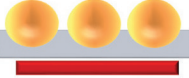

The following example, summarized in Table 2, is presented to illustrate how heat pipes might be used to solve a thermal challenge for 70 W heat source with dimensions 20 mm x 20mm and a single 90 degree heat pipe bend required to transport heat from evaporator to condenser. Furthermore, the heat pipes will operate in a horizontal position.

- To be at their most effective, heat pipes need to fully cover the heat source, which in this case is 20 mm wide. From Table 1, it appears that there are two choices: three round 6 mm pipes or two flattened 8 mm pipes. Remember the three 6 mm configuration will be placed in a mounting block with 1 to 2 mm between the heat pipes.
- Heat pipes can be used in conjunction to share the heat load. The 6 mm configuration has a  $Q_{\max}$  of 114W (3 x 38 W), while the flattened 8 mm configuration has a  $Q_{\max}$  of 104 W (2 x 52 W).
- It's just good design practice to build in a safety margin, and it is suggested to typically use 75% of rated  $Q_{\max}$ . Therefore select 85.5W for the 6 mm (75% x 104 W) and 78 W for the 8 mm (75% x 104 W)
- Finally the influence of bending needs to be accounted for. A 90 degree bend will reduce  $Q_{\max}$  of each configuration by another 5%. The resulting  $Q_{\max}$  for the 6 mm configuration is therefore just over 81 W and for the 8 mm configuration it is 74 W, both of which are higher than the 70 W heat source that is to be cooled.

As can be seen from this analysis, both heat pipe configurations are adequate to transport heat from the evaporator to the condenser. So why choose one over the other? From a mechanical perspective it may simply come down to heat sink stack height at the evaporator, i.e. the 8 mm configuration has a lower profile than does the 6mm configuration. Conversely, condenser efficiency

may be improved by having heat input in three locations versus two locations, necessitating the use of the 6 mm configuration.

**Table 2. Heat pipe configuration options for a 20 mm x 20 mm heat source dissipating 70 W.**

Parameter	Configuration	
Heat pipe geometry		
	6 mm circular	8 mm flat
Required heat pipe bend	One 90°	One 90°
Number of heat pipes	Three round 6 mm	Two 8 mm flattened to 2.5mm
Heat pipe width as configured	20mm = 18 mm + 2 x 1 mm gap in baseplate	22.3 mm = 2 x 11.14 mm
$Q_{\max}$ per heat pipe as configured	38 W	52 W
$Q_{\max}$ as configured	114 W	104 W
25% $Q_{\max}$ safety margin	85.5 W	78 W
Less 5% $Q_{\max}$ for bend	81 W	74 W

## 5.0 HEAT SINKS

There are numerous choices from zipper pack fins to extruded fin stacks, each with their own cost and performance characteristics. While heat sink choice can markedly affect heat dissipation performance, the biggest performance boost for any type of heat exchanger comes with forced convection. *Table 3* compares the benefits and pitfalls for range of heat sinks, some of which are illustrated in *Figure 5*.

**Table 3. Heat pipe selection considerations for a condenser heat sink.**

Heat Sink	Cost	Typical Benefits	Potential Pitfalls
Extruded	\$	<ul style="list-style-type: none"> <li>Readily available</li> <li>Easy to manufacture to custom specifications, including grooves for heat pipes</li> </ul>	<ul style="list-style-type: none"> <li>Dimensions are limited</li> <li>Fin height limited ~20x fin width</li> <li>Base and fins are same material, usually aluminum</li> </ul>
Die Cast	\$	<ul style="list-style-type: none"> <li>Net shape</li> <li>Low weight</li> <li>Easily customizable</li> </ul>	<ul style="list-style-type: none"> <li>Lower thermal conductivity</li> <li>Potential for porosity</li> <li>Not generally used with heat pipes</li> </ul>
Bonded	\$\$	<ul style="list-style-type: none"> <li>Large heat sink sizes</li> <li>Base and fins can be of different materials</li> </ul>	<ul style="list-style-type: none"> <li>If fins are epoxied in place, added thermal resistance</li> </ul>
Skived	\$\$	<ul style="list-style-type: none"> <li>Fin and base from solid piece of metal, usually copper</li> <li>High density fins possible</li> <li>More design flexibility than extrusion</li> </ul>	<ul style="list-style-type: none"> <li>Base may be thicker than needed, thus higher weight</li> <li>Fins damage easily</li> </ul>
Fin Pack and Zipper Fins	\$\$	<ul style="list-style-type: none"> <li>Low-high fin density</li> <li>Low weight</li> <li>High design options, including center mounted heat pipes</li> </ul>	<ul style="list-style-type: none"> <li>Generally, for fins less than 1mm thick</li> </ul>
Forged	\$\$\$	<ul style="list-style-type: none"> <li>Fin design in many shapes (pin, square, oval, etc.)</li> </ul>	<ul style="list-style-type: none"> <li>Usually reserved for higher volume products as tooling is expensive</li> </ul>
Machined	\$\$\$\$	<ul style="list-style-type: none"> <li>High thermal conductivity</li> <li>Complicated designs OK</li> </ul>	<ul style="list-style-type: none"> <li>None, other can cost.</li> <li>Not good for high volume due to production time</li> </ul>

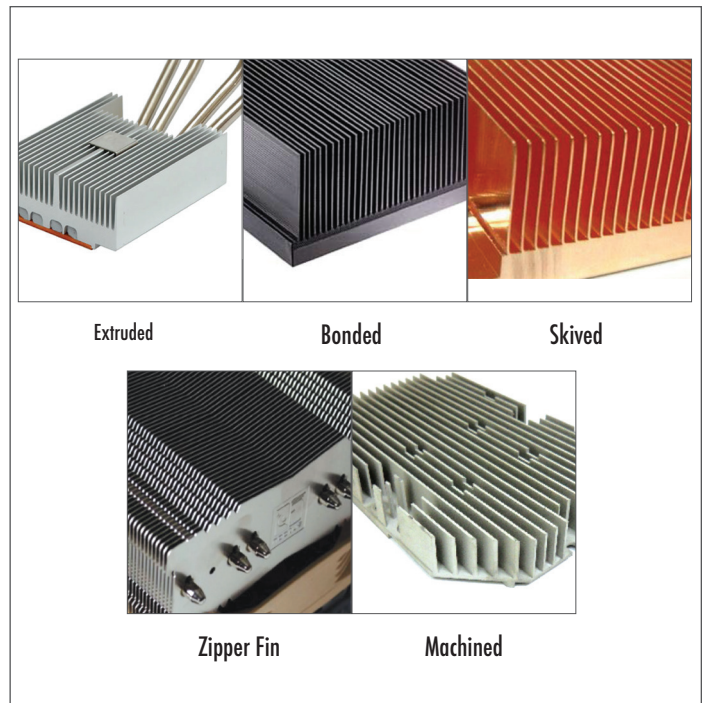


**Figure 5. Heat sink designs whose characteristics are summarized in Table 3.**

As a starting point for determining heat sink selection, *Equation (2)* can be used to estimate the required heat sink volume for a given application:

$$V = Q R_v / \Delta T \quad (2)$$

where:  $V$  = heat sink volume [ $\text{cm}^3$ ],  $Q$  = heat to be dissipated [W],  $R_v$  = volumetric thermal resistance [ $\text{cm}^3\text{-}^\circ\text{C}/\text{W}$ ],  $\Delta T$  = maximum allowable temperature difference [ $^\circ\text{C}$ ].

*Table 4* provides guidance on the range of heat sink volumetric thermal resistances as a function of air flow conditions.

**Table 4. Typical heat sink volumetric thermal resistance range as function of air flow conditions [6].**

Air Flow (m/s)	Volumetric Thermal Resistance ( $\text{cm}^3\text{-}^\circ\text{C}/\text{W}$ )
Natural Convection	500 - 800
1 m/s (gentle air flow)	150 - 250
2.5 m/s (moderate air flow)	80 - 150
5 m/s (high air flow)	50 - 80

Whether dealing with a heat exchanger that is local or remote to the heat source, the options for mating heat pipes to them are identical and include grooved base, grooved mounting block and direct contact methods as illustrated in *Figure 6*.



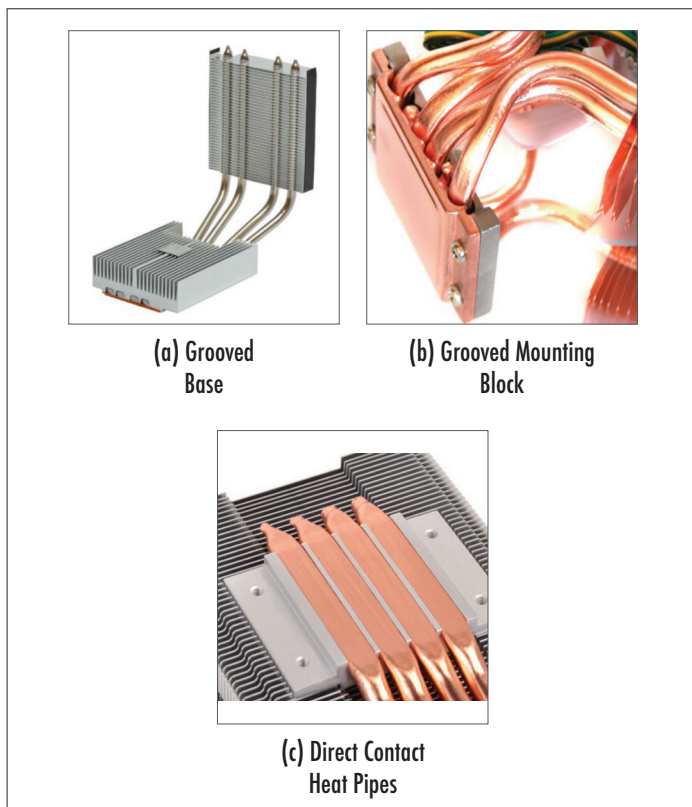


Figure 6. Heat pipe condenser mating.

It should go without saying that simply soldering a round pipe to a flat surface is far from optimal. Circular or semi-circular grooves should be extruded or machined into the heat sink. It's advisable to size the grooves about 0.1 mm larger than the diameter of the heat pipe in order to allow enough room for the solder.

The heat sink shown in *Figure 6(a)* uses both a local and remote heat sink. The extruded heat exchanger is designed to accommodate slightly flattened heat pipes, helping to maximize the contact between the copper mounting plate and the heat source. A remote stamped fin pack is used to further increase thermal performance. These types of heat exchanger are particularly useful because the pipes can run directly through the center of the stack, decreasing conduction loss across the fin length. Because no base plate is required with this fin type, weight and cost can be reduced. Again the holes through which the heat pipes are mounted should be 0.1 mm larger than the pipe diameter. Had the pipe been completely round at the heat source, a thicker grooved mounting plate would have been required as seen in *Figure 6(b)*

If conduction losses due to the base plate and extra TIM layer are still unacceptable, further flattening and machining of the heat pipes allows direct contact with the heat source as seen in *Figure 6(c)*. Performance gains from this configuration usually lead to between a 2-8 °C reduction in temperature rise. In cases where direct contact of the heat source to the

heat pipes is required a vapor chamber, which can also be mounted directly, should be considered due to its improved heat spreading capacity.

The primary reason for considering a heat pipe solution is improved performance. As such, the use of thermal tape or epoxy as the primary means of attaching the heat sink to the die is not suitable. Instead three types of mechanical attachments are often used with heat pipes; all of which can meet MIL-810 and NEBS Level 3 shock and vibration requirements.

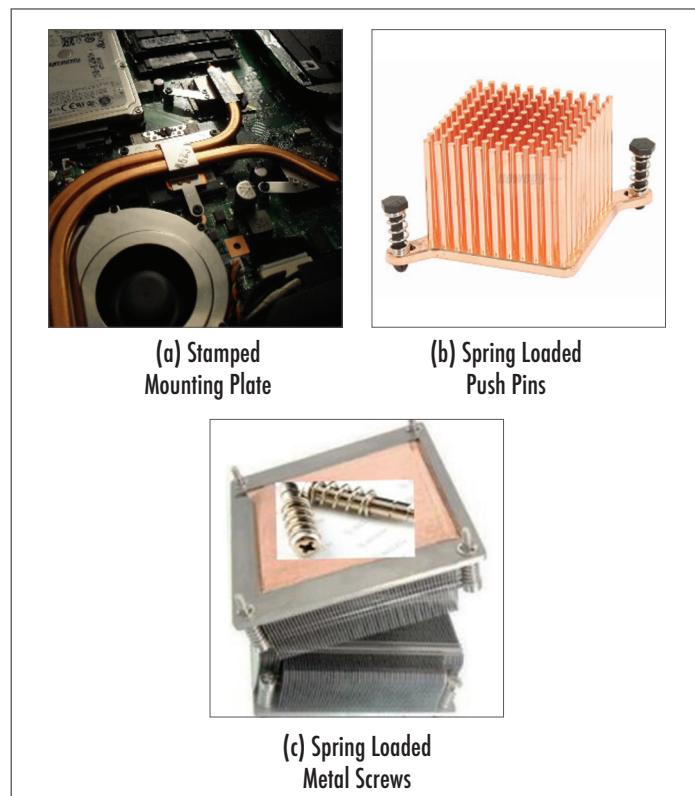


Figure 7. Heat pipe attachment methods for small (low mass) heat sinks.

Finally, typical heat pipe attachment methods for small (low mass) heat sinks are shown in *Figure 7*. In *Figure 7(a)* a stamped mounting plate is shown. Although it requires two PCB holes, this method offers better shock and vibration protection relative to thermal tape or epoxy, and some TIM compressions – with up to 35 Pa compression required. *Figure 7(b)* shows spring loaded plastic or steel push pins further increase TIM compression up to around 70 Pa. Installation is fast and simple but removal requires access to the back of the PCB. Push pins should not be considered for anything more than light duty shock and vibrate requirements. Spring loaded metal screws, *Figure 7(c)*, offer the highest degree of shock and vibration protection as they are the most secure method of attaching a heat sink to the die and PCB. They offer the highest TIM preload at approximately (520 Pa).

## SUMMARY

Design guidance was provided on the use copper tube heat

pipes with sintered copper wick using water as the working fluid. As outlined, heat pipe selection needs to consider a range of factors including effective thermal conductivity, internal structure and physical characteristics, in addition to the heat sink characteristics.

## REFERENCES

- [1] Garner, S.D., "Heat Pipes for Electronics Cooling Applications," *ElectronicsCooling*, September 1996, <http://www.electronics-cooling.com/1996/09/heat-pipes-for-electronics-cooling-applications/>, accessed August 15, 2016.
- [2] Graebner, J.E., "Heat Pipe Fundamentals," *ElectronicsCooling*, June 1999, <http://www.electronics-cooling.com/1999/05/heat-pipe-fundamentals/>, accessed August 15, 2016.
- [3] Zaghdoudi, M.C., "Use of Heat Pipe Cooling Systems in the Electronics Industry," *ElectronicsCooling*, December 2004, <http://www.electronics-cooling.com/2004/11/use-of-heat-pipe-cooling-systems-in-the-electronics-industry/>, accessed August 15, 2016.

[4] Peterson, G.P., *An Introduction to Heat Pipes: Modeling, Testing and Applications*, John Wiley & Sons, New York, US, (1994).

[5] Meyer, G., "How Does Bending Affect Heat Pipe & Vapor Chamber Performance?" November, 2015, <http://celsiainc.com/blog-how-does-bending-affect-heat-pipe-vapor-chamber-performance/>, accessed August 15, 2016.

[6] Meyer, G., "Design Considerations When Using Heat Pipes (Pt. 2)," August 2016, <http://celsiainc.com/design-considerations-when-using-heat-pipes-pt-2/>, accessed August 15, 2016.

## CONTACT INFORMATION:

**George Meyer**

CEO

Celsia Inc

3287 Kifer Road, Santa Clara CA, 95051

Email: [gmeyer@celsiainc.com](mailto:gmeyer@celsiainc.com)

# ECTC 2017

The 67th Electronic Components  
and Technology Conference

## May 30 - June 2, 2017

Walt Disney World Swan & Dolphin Resort  
Lake Buena Vista, Florida, USA

As the premier event in the semiconductor packaging industry, ECTC addresses new developments, trends and applications for 3D integration, TSV, WLP, flip-chip, photonics, LED, materials and other integrated systems packaging topics.

Abstract submissions and Professional Development Course proposals for the 67th ECTC are due by **October 10, 2016.**

To submit, visit:  
**[www.ectc.net](http://www.ectc.net)**

Conference Sponsors:



## Call for Papers Opens August 8!

We welcome previously unpublished, non-commercial abstracts in areas including, but not limited to:

**Advanced Packaging**  
**Applied Reliability**  
**Assembly & Manufacturing Technology**  
**Emerging Technologies**  
**High-Speed, Wireless & Components**  
**Interconnections**  
**Materials & Processing**  
**Thermal/Mechanical Simulation & Characterization**  
**Optoelectronics**



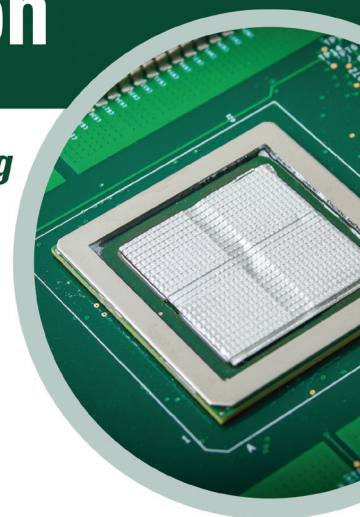
# Index of ADVERTISERS

Alpha Novatech, Inc.....	Back Cover
The Bergquist Company .....	Inside Front Cover
CD Adapco Group.....	33
Delta Products Corporation .....	27
ECTC .....	39
Electronics Cooling .....	28
Electronica .....	21
International Manufacturing Services.....	16
Indium Corporation.....	40
Malico Inc. (Enzotechnology Corp.).....	12
Master Bond, Inc.....	15
Mentor Graphics .....	17
SEMI-THERM .....	Inside Back Cover
Thermal Live 2016 .....	3
Thermal Live Sneak Peak.....	6-7

## Thermal Voiding Solution

***Thermal voiding  
causes  
hot spots.***

***Hot spots  
spell disaster  
to your device.***



**Heat-Spring® metal-based  
thermal interface materials  
help you Avoid the Void.™**

- No pump out
- No bake out
- Thermal conductivity as high as 86W/mK
- Easily placed for proper coverage
- Maximized contact area
- Available in indium, indium alloys, Sn+, and other metals

Contact our technical engineers today:

**[techsupport@indium.com](mailto:techsupport@indium.com)**

Learn more: [www.indium.com/TIM](http://www.indium.com/TIM)

**From One  
Engineer  
To Another®**

**[cgowans@indium.com](mailto:cgowans@indium.com)**



ASIA • CHINA • EUROPE • USA

©2016 Indium Corporation



Thermal Innovations that Make the World's Technology Cool  
Thermal Measurement, Modeling and Management Symposium and Exhibition

THIRTY-THIRD ANNUAL  
**CALL FOR PAPERS**

March 13-17, 2017

DoubleTree by Hilton, San Jose, CA, USA

SEMI-THERM is an international forum dedicated to the thermal management and characterization of electronic components and systems. It provides knowledge covering all thermal length scales from IC to facility level. The symposium fosters the exchange of knowledge between thermal engineers, professionals and leading experts from industry as well as the exchange of information on the latest academic and industrial advances in electronics thermal management. Areas of interest include, but are not limited, to the following:

Topics:

- Component, Board- and System-Level Thermal Design Approaches
- Air Mover Technologies with Low Acoustics
- Thermal Integration in the Product Design Process
- Multi-Physics Based Reliability, including Accelerated Testing
- Multi-objective Design and Optimization, Modeling and Characterization
- Novel Materials: Heat Spreaders, Thermal Vias and Thermal Interface Materials
- Nanotechnology: Thermal, Mechanics, Material and Process Related Issues In Nanostructures
- Micro-Fluidics
- Characterization and Standardization of Material Property Measurements
- Energy Harvesting Materials, Thermo-electrics
- Novel and Advanced Cooling Techniques/Technology
- Roadmaps, Specifications and Traditional Cooling Limits
- Mechanical Modeling, Simulations and Characterization
- Characterization and Modeling of Multi-Scale Heat Transfer Problems
- Computational Fluid Dynamics (CFD) Analysis and Validation
- Multi-physics Modeling and Characterization of Products and Processes
- Thermal Control Methodologies

Application areas:

- Processors, ICs, and Memory
- 3-D Electronics
- Wireless, Network, Computing Systems
- Data Centers
- Portable and Consumer Electronics
- Power Electronics
- Harsh Environments
- Commercial, Defense, and Aerospace Systems
- Solid-State Lighting
- Solid State Energy Generation/Cooling
- Medical and Biomedical electronics
- Instrumentation and Controls
- Micro- and nano-scale devices
- MEMS and sensors
- Alternative and Renewable Energy
- Wearables

**To submit an extended abstract**

You are invited to submit an extended abstract describing the scope, contents, key results, findings and conclusions. This abstract of 2 to 5 pages is supported by figures, tables and references as appropriate. Abstracts must demonstrate high technical quality, originality, potential impacts. Upload your abstract electronically in RTF, DOC or PDF formats at **[www.semi-therm.org](http://www.semi-therm.org)**

Abstract Submission Deadline: September 26, 2016

Abstract Acceptance Notification: November 3, 2016

Photo-ready Full Manuscript Due: January 6, 2017

**To submit a peer-reviewed paper**

You are invited to submit a full paper to be reviewed by the SEMI-THERM Technical Committee. Papers must include a one paragraph abstract and keywords and must demonstrate high technical quality, originality, and potential impacts. Special consideration is given to papers based on academic/industry cooperation projects. Upload your paper electronically in RTF, DOC or PDF formats at **[www.semi-therm.org](http://www.semi-therm.org)**

Peer-Reviewed Paper Submission Deadline: September 26, 2016

Peer-Reviewed Paper Acceptance Notification: November 3, 2016

Photo-ready Full Manuscript Due: January 6, 2017



# Alpha's Next Generation Heat Sinks

Custom or off-the-shelf.

Simple to complex.

Prototype to mass production.

## Shoulder Screw Heat Sinks

### Off-the-shelf heat sinks with attachment holes

Multiple base size & height options are available. We can design and ship the entire heat sink assembly, including captive screws, springs, and interface material the same day!

### Easy selection process

Online design tools allow for simple selection of the shoulder screw, spring, and thermal interface material.

### Simple & Robust

Extremely reliable and robust attachment. Screws & springs are captive to the heatsink, so installation is safe & simple.

### Prevent board warpage

Optional backing plate can be used to prevent excessive PCB warpage under high attachment load.

# ALPHA

Your partner for thermal solutions

ALPHA Co., Ltd.  
Head Office  
[www.micforg.co.jp](http://www.micforg.co.jp)

256-1 Ueda, Numazu City, Japan 410-0316  
Tel: +81-55-966-0789 Fax: +81-55-966-9192  
Email: [alpha@micforg.co.jp](mailto:alpha@micforg.co.jp)

ALPHA NOVATECH, INC.  
USA Subsidiary  
[www.alphanovatech.com](http://www.alphanovatech.com)

473 Sapena Ct. #12, Santa Clara, CA 95054 USA  
Tel: +1-408-567-8082 Fax: +1-408-567-8053  
Email: [sales@alphanovatech.com](mailto:sales@alphanovatech.com)